Environmental Health Perspectives
Vol. 64, pp. 233-252, 1985

Free Radical Generation by Ultrasound in Aqueous and Nonaqueous Solutions

by P. Riesz,* D. Berdahl,† and C. L. Christman‡

The physical principles underlying the oscillatory behavior of minute gas bubbles in liquids exposed to ultrasound are reviewed. Results from mathematical analyses suggest that these oscillations sometimes become unstable leading to transient cavitation in which a bubble violently collapses during a single acoustic half-cycle producing high temperatures and pressures. The role that micronuclei, resonant bubble size, and rectified diffusion play in the initiation of transient cavitation is explained. Evidence to support these theoretical predictions is presented with particular emphasis on sonoluminescence which provides some non-chemical evidence for the formation of free radicals. Acoustic methods for conducting sonochemical investigations are discussed.

In aqueous solutions transient cavitation initially generates hydrogen atoms and hydroxyl radicals which may recombine to form hydrogen and hydrogen peroxide or may react with solutes in the gas phase, at the gas–liquid boundary or in the bulk of the solution. The analogies and differences between sonochemistry and ionizing radiation chemistry are explored. The use of spin trapping and electron spin resonance to identify hydrogen atoms and hydroxyl radicals conclusively and to detect transient cavitation produced by continuous wave and by pulsed ultrasound is described in detail.

The study of the chemical effects of cavitation in organic liquids is a relatively unexplored area which has recently become the subject of renewed interest. Examples of the decomposition of solvent and solute, of ultrasonically initiated free-radical polymerization and polymer degradation are presented. Spin trapping has been used to identify radicals in organic liquids, in polymer degradation and in the decomposition of organometallic compounds.

Introduction

When an ultrasonic wave propagates through a liquid, the local pressure varies with time and space. If a bubble is present in the liquid, its radius will expand and contract in response to these pressure changes. For low amplitude pressure excursions, these oscillations are sinusoidal and may last for many acoustic cycles, a phenomenon called stable cavitation. Under certain conditions, however, these oscillations may become unstable leading to the rapid collapse of a bubble during a single acoustic half-cycle. This phenomenon is called transient cavitation. High temperatures and pressures are generated within the bubble during its final stage of collapse that are thought to produce hydrogen atoms and hydroxyl radicals in aqueous solutions. Some investigators feel that temperatures sufficient to generate free radicals are sometimes produced for stable cavitation as well.

*Radiation Oncology Branch, Clinical Oncology Program, Division of Cancer Treatment, National Cancer Institute, National Institutes of Health, Bethesda, MD 20892.

†Chemical and Engineering Laboratory, General Electric Corporation, Research and Development Center, One River Road, Schenectady, NY 12345.

‡Acoustic Radiation Branch, Division of Life Sciences, Office of Science and Technology, Center for Devices and Radiological Health, 12709 Twinbrook Parkway, Rockville, MD 20857.

In this review article, we will first outline the theoretical basis for cavitation and will discuss its implication for investigators conducting sonochemical studies. Then we will present chemical evidence for the formation of $^{\cdot}H$ and $^{\cdot}OH$ that includes the detection of chemical products formed in solution and more directly using spin-trapping and electron spin resonance (ESR) techniques. As an extension to the results obtained in aqueous solutions, we will present evidence for the formation of free radicals in organic solutions, as well. This evidence will include examples of the decomposition of solvents and solutes, of free radical polymerization and of polymer degradation.

Cavitation

Interest in cavitation, which occurs whenever a new gas or vapor filled cavity forms in a liquid, dates back at least 125 years. Even today, this topic has broad appeal since it is studied for a variety of applications that include hydraulics, sonar propagation, decompression sickness, sonochemistry and bio-medical ultrasonics. We will attempt to focus our discussion on the sonochemical implications of cavitation with particular emphasis on how this phenomenon gives rise to the production of free radicals. For interested readers who want a more complete discussion, numerous review ar-

ticles are available, each with their own particular emphasis (*1–5*).

Flynn prepared the first comprehensive review of the theoretical aspects of cavitation and his chapter still serves as an excellent source of basic information (*1*). A more recent review of cavitation, written by Apfel, is particularly strong on the mathematical treatment of bubble dynamics (*2*). A safety standard, with a good explanation of cavitation and complete definitions of acoustic intensity parameters, is also available (*3*). Coakley and Nyborg's review is particularly useful for those interested in biomedical applications (*4*). For those interested in sonochemistry, Basedow and Ebert discuss how cavitation is involved in sonically induced degradation of polymers (*5*).

Neppiras provides a clear, concise introduction to cavitation that offers unambiguous definitions for many of the terms needed for this discussion (*6*). He considers cavitation to occur when a new cavity is created within a liquid. This cavity may contain gas or vapor or may be a void. This broad definition includes phenomena such as boiling and effervescence that only involve expansion of the gas phase. The term acoustic cavitation refers to the expansion and contraction of cavities, also referred to as bubbles, due to the passage of acoustic waves through the liquid.

Cavitation has been conveniently classified into two types, stable and transient. Stable cavities are bubbles that oscillate radially about some equilibrium size and often will persist for many acoustic cycles. Transient cavities, on the other hand, exist for only one or two acoustic cycles and will expand to at least two to three times their original size during the negative acoustic pressure half-cycles before violently collapsing during a single compression half-cycle. During the final stage of collapse, the velocity of the liquid gas interface approaches the speed of sound in the liquid and the temperature and pressure within the cavity will become enormous ($> 3{,}000$°K and $> 10{,}000$ bar, where 1 bar $= 10^5$ Pa ≈ 1 atm).

Since these temperatures are thought to be responsible for the generation of free radicals, for which chemical evidence will be discussed later, we will be primarily concerned with transient cavitation. This is not a mutually exclusive topic though since stable cavitation bubbles may sometimes grow by a process called rectified diffusion and become transformed into transient bubbles. Transient cavitation can therefore be regarded as a complex process that can be conveniently divided into three stages: nucleation, growth, and collapse.

When an acoustic longitudinal wave propagates through a liquid, the total external pressure, $P(t)$, experienced by a macroscopic volume element is composed of two parts, a static part and a time varying part. Thus, $P(t)$ is given by:

$$P(t) = P_0 + P_A \sin(\omega t) \tag{1}$$

where P_0 is the static pressure (usually the atmospheric pressure), P_A is the maximum amplitude of the acoustic pressure, and ω is the angular frequency of the acoustic wave. The intensity I of ultrasound, defined here as an acoustic wave whose frequency is greater than 20 kHz, is given by:

$$I = P_A^2/2\rho c \tag{2}$$

where ρ is the density and c is the velocity of sound. The product ρc is called the acoustic impedance of the liquid.

For illustration, consider a 1.0 MHz ultrasonic wave with a spatial peak temporal average (SPTA) intensity of 3 W/cm^2 propagating through water at 30 °C. From Eq. (2), P_A is calculated to be 3.0 bar, assuming $\rho = 1.0$ g/cm^3 and $c = 1500$ m/sec. Thus, the dynamic pressure varies from 3.0 to -3.0 bar one million times per second. This example shows that even for moderate acoustic intensities, the liquid will be in tension, as represented by a negative external pressure, during part of the acoustic cycle, assuming the static pressure is 1 bar (normal atmospheric pressure).

The tension produced by ultrasound is ultimately responsible for producing cavitation. Assuming intramolecular forces within the liquid must be overcome to produce a new cavity, as required by the homogeneous nucleation theory, the cavitation threshold for water should be between -1300 and -1500 bar (*7*). Experimental results indicate a much lower value which can be increased by careful preparation of the liquid. Greenspan and Tschiegg reported a threshold for clean water ranging from -160 bar for 1-min observation intervals to -210 bar for observation intervals of a few seconds (*8*). Cavitation was detected as an audible pop or by direct visual observation using a darkfield microscope. In a related experiment, Apfel measured the cavitation threshold of filtered 0.5 mm droplets of ether acoustically levitated in glycerine and was able to confirm the homogeneous nucleation theory (*9*).

Since water's ultimate tensile strength has never been observed, some inhomogeneities, usually referred to as cavitation micronuclei, must exist to explain why water ruptures so easily. These inhomogeneities can not be free bubbles though, since bubbles are inherently unstable and will rise to the surface due to buoyancy or will shrink and eventually collapse due to surface tension. Neglecting vapor pressure and assuming saturation of gas within the liquid, the pressure P_i inside a static bubble is given by:

$$P_i = P_0 + (2\sigma/R) \tag{3}$$

where σ is the surface tension and R is the radius of the bubble. To be in equilibrium, the pressure inside a bubble must be larger than the pressure outside causing a net diffusion of gas out of the bubble.

Several models have been proposed to explain how gas bubbles can be stablized in a liquid (*10*). One of the earliest of these was the crevice model, shown schematically in Figure 1. A partially wetted solid impurity, called a mote, contains a gas-filled crevice with an apex

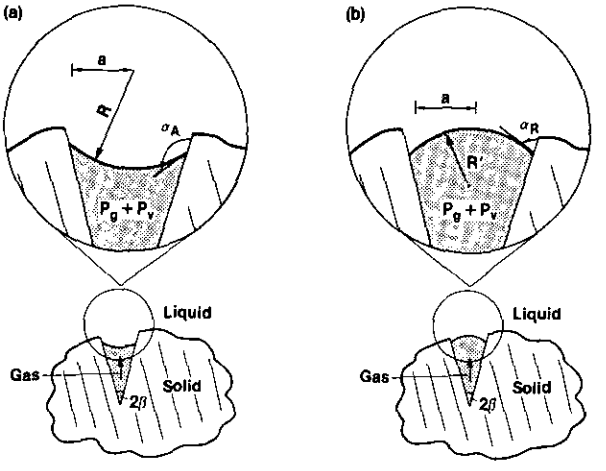

FIGURE 1. Crevice model for stabilizing cavitation micronuclei: (*a*) for external positive pressure; (*b*) for external negative pressure.

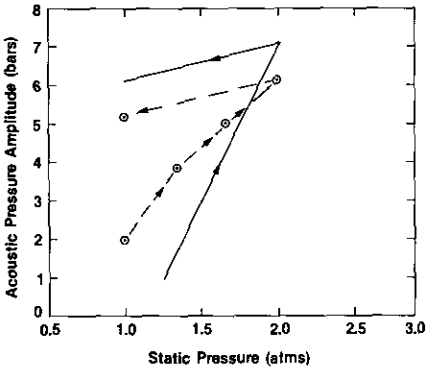

FIGURE 2. Variation of cavitation threshold with static pressure: (--) experimental data; (——) prediction of crevice model. Arrows indicate the direction of pressure change.

angle of 2β. P_g and P_v represent the equilibrium gas pressure and vapor pressure within the crevice, respectively. Assume initially, the liquid gas interface is concave towards the apex, as shown in Figure 1*a*. Note this represents a stable state, since the surface tension term in Eq. (3) is negative for this case.

When an external pressure is applied, such as from a time varying acoustic wave, the contact angle α increases until it reaches its maximum value α_A, the advancing contact angle. If the pressure is increased further, the interface moves toward the apex and may completely disappear if the pressure is sufficiently high. When the pressure is decreased, the interface becomes convex as shown in Figure 1*b*, and will eventually reach its minimum value α_R, the receding contact angle. A further decrease in pressure causes the interface to move away from the apex and if the pressure becomes sufficiently low, a free gas bubble will be liberated. This process is called nucleation.

Apfel estimates that ordinary tap water contains as many as 100,000 motes/cm^3 (*11*). If motes are less than 10 μm in diameter, Brownian motion has a greater effect than gravitational forces and the motes become permanently suspended in the liquid. Apfel derived a cavitation threshold pressure based on this model, that predicts the threshold strongly depends on gas saturation for large crevices but for small crevices, the gas dependence is small (*12*). This result agrees with the data of Greenspan and Tschiegg, who found little gas dependence when large particles were removed by filtering (*8*).

Crum modified Apfel's model using a relationship between the equilibrium contact angle and surface tension. Using values for β, α_A, and α_R, partially obtained from the literature and partially chosen to give the best fit to the experimental data, he was able to correctly predict the variation of cavitation threshold for water at 36 kHz as a function of temperature, equilibrium gas concentration and surface tension (*13*). The model correctly predicted the remarkable result that lower surface tensions gave significantly higher cavitation thresholds.

The crevice model is also useful for explaining the hysteresis effect of pressurization on cavitation threshold. Using a spherical resonator, Strasberg measured the cavitation threshold at 550 kHz by visual observation as a function of static pressure (*14*). His results are shown by the circles and dashed lined in Figure 2. The arrows indicate the direction of pressure change. Using the crevice model, Crum predicts the variation of cavitation threshold with static pressure to be the solid curve, in reasonably good agreement with the experimental results (*13*). The cavitation threshold increases because pressurization causes the crevice to shrink and gas diffuses into the liquid. After the pressure is released, a smaller pocket of gas exists in the crevice requiring a greater negative acoustic pressure to produce nucleation.

Another model to explain the stabilization of cavitation micronuclei suggests that a film of surface-active substances exists on the liquid gas interface. This model was originally proposed by Fox and Herzfeld as a rigid-skin model (*15*) but was later abandoned. It has since been reintroduced and supported by Sirotyuk with new experimental data (*16,17*). In this model an organic skin is composed of molecular chains each containing both a polar and a nonpolar end. The polar end bonds to the water surface while the nonpolar end extends into the gas. The alignment of molecules in this "picket fence" arrangement has some elasticity that stabilizes the bubble. Sirotyuk found that his threshold for growth by rectified diffusion, a phenomenon that will be discussed later, increased by a factor of 4 when all but trace amounts of surface-active substances were removed.

Yount has proposed a modification that allows the skin to be initially permeable but to become impermeable when the pressure is raised above some critical value (*18*). This modification allows the model to predict results that agree with experimental data involving gas diffusion and static pressure changes. Although Yount's

model was originally used to explain bubble formation in gelatin upon rapid decompression, he believes it is a general phenomena that applies to bubbles in water as well. Since surfactants are prevalent in biological systems, this model may be particularly important for applications involving decompression sickness and medical ultrasonics.

Numerous theories are available to explain how cavitation micronuclei are stabilized. Perhaps situations exist when some combination of the models will be needed to explain the experimental results. At the present time, because of uncertainties in the parameters on which the models depend, additional experiments are needed before a definitive statement can be made about the source of cavitation micronuclei (*11*).

Cavitation micronuclei are not always permanently stabilized. Short-lived micronuclei can also be formed by radiation. Greenspan and Tschiegg showed that after cleaning water to raise its cavitation threshold to −160 bar, the threshold could be lowered again to −50 bar by irradiating with 10 MeV neutrons (*8*). Although many theories have been proposed to explain these results, the one that seems to have the most experimental support is the thermal spike model (*19*). In this model, a positive ion is created by the radiation-matter interaction. This ion quickly liberates its energy, producing neighboring atoms that are thermally excited. If tension exists within the liquid, due to an acoustic pressure wave for example, this region can produce a vapor bubble that expands and eventually results in a cavitation event. Bubbles also form in superheated liquids this way, in the absence of ultrasound, as illustrated by the operation of an ordinary bubble chamber.

For transient cavitation to occur after a free bubble has been nucleated, it must first grow. This is accomplished by radial oscillations of the liquid gas interface in a manner that is analogous to a mass spring system, as shown in Figure 3 (*20*). Apfel provides a relatively simple derivation for an equation to describe the time dependence of R, the radius of the liquid–gas interface. His result is given by:

$$RR'' + \frac{3(R')^2}{2} + \frac{4\mu R'}{\rho R} + \frac{2\sigma}{\rho R} = \frac{P_i - P(t)}{\rho} \qquad (4)$$

where μ is the viscosity of the liquid and $R' = dR/dt$. The first two terms are inertial terms, the third term is needed to account for viscous losses, and the remaining terms account for surface tension and pressure effects. The liquid is assumed to be incompressible, the gas content of the bubble is assumed to remain constant and the diameter of the bubble is assumed to be much less than an acoustic wavelength so that the pressure within the bubble P_i will be constant at any given time.

Noltingk and Neppiras found by neglecting viscosity and considering only small steady-state oscillations, as occurs for stable cavitation, Eq. (4) reduces to the form of a forced harmonic oscillator (*21*). Such a system has a natural resonance frequency which in this case is given by:

$$f = \frac{1}{2\pi R_r}\left[\frac{3KP_o}{\rho}\left\{1 + X_r\left(1 - \frac{1}{3K}\right)\right\}\right]^{1/2} \qquad (5)$$

where

$$X_r = \frac{2\sigma}{P_o R_r}$$

and

$$f = \frac{1}{2\pi R_r}\left(\frac{3KP_o}{\rho}\right)^{1/2} \quad \text{for } X_r << 1 \qquad (6)$$

using the notation of Apfel (*2*). R_r is the resonance radius and K is the exponent which varies between 1.0, when the oscillations are adiabatic, and γ, when the oscillations are isothermal, where γ is the ratio of specific heats for the liquid. Equation (5) predicts that at 1.6 MHz the resonance radius of an air bubble in water at 30°C is about 2 μm. Figure 4 is a plot of the resonance radius of an air bubble in water at 30°C, as a function of driving frequency (*22*). The solid curve represents the results for Eq. (5), while the dashed line represents the results for its simplified form which neglects surface tension [Eq. (6)]. As shown, surface tension only becomes important for frequencies above 1.0 MHz.

One consequence of small radial oscillations, also referred to as stable cavitation, is the growth of a bubble by a process called rectified diffusion. During the compressional phase of the acoustic cycle, the bubble will shrink causing gas to diffuse out of the bubble. During

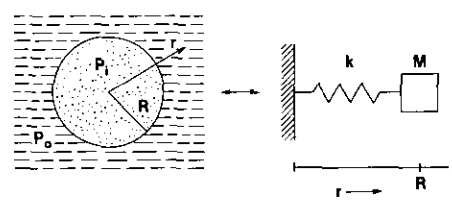

FIGURE 3. Mass spring analogy for a gas bubble in water.

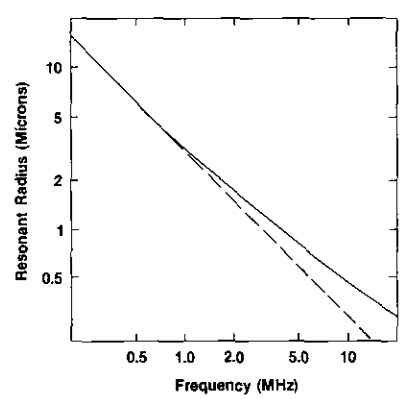

FIGURE 4. Variation of resonant radius with frequency for an air bubble in water: (--) results that neglect surface tension; (——) results including the effect of surface tension.

the rarefaction phase of the cycle, on the other hand, the bubble expands causing gas to diffuse into the bubble. Since the surface area is larger when the bubble expands, a net increase of gas in the bubble occurs. This process competes with the natural tendency for the bubble to shrink. For certain critical conditions that depend on bubble size, the intensity of ultrasound and the concentration of dissolved gas in the liquid, bubbles below resonance size will grow. The threshold intensity for bubble growth can be very small (6 mW/cm^2 at 1.0 MHz) for bubbles near resonance size (*4*). This growth usually occurs rapidly. For air bubbles in water at a driving frequency of 1.0 MHz, bubbles will grow through resonance within 10 msec (*23*).

The bubbles formed by stable cavitation may be trapped at certain fixed locations by the effects of acoustic radiation force, which is proportional to the negative gradient of the pressure field. Consider a standing wave exposure field produced when an incident plane wave is reflected at normal incidence from an interface. The interference between these two plane waves, that are traveling in opposite directions, produces a new time variant pressure field whose magnitude depends on a spatial coordinate. The plane of minimum pressure is called a pressure node (or displacement antinode) while the plane of maximum pressure is called a pressure antinode. Radiation forces will propel bubbles smaller than resonance size to pressure maxima while bubbles larger than resonance size move to pressure minima. These forces often play an important role in cavitation detection especially for resonator systems. For example, Crum has observed that small bubbles move toward a pressure antinode, grow in size by rectified diffusion and shoot away from the antinode after becoming larger than resonance size (*13*).

Now that we have discussed nucleation and bubble growth due to stable cavitation, we will turn our attention to transient cavitation. For radical oscillations of a small bubble, Eq. (4) proved useful for predicting its resonant bubble size. This same equation has also been used to predict bubble dynamics for larger radial oscillations that are characteristic of transient cavitation. The results from numerical methods predict that when the driving pressure is significantly high, the bubble initially at radius R_o will grow for a few acoustic cycles until it reaches a maximum value R_m that is at least two to three times its initial radius (*2*). Then it will collapse during the next acoustic compression halfcycle. Assuming an adiabatic collapse, which may be reasonable considering the short collapse time, the final temperature of the gas within the bubble is approximated by:

$$T_f = T_o\,(R_m/R_f)^{3(\gamma-1)} \qquad (7)$$

when T_o is the temperature of the liquid and R_f is the final bubble radius (*21*). Although Eq. (7) is an oversimplified approximation, it is useful for demonstrating that enormous temperatures should be generated during a bubble's collapse since this temperature is proportional to the cube of its fractional change in radius.

Apfel has investigated the validity of using Eq. (4) under these conditions (*2*). He concludes that it is valid until the final stage of collapse when the initial assumption of an incompressible liquid is violated as the velocity of the liquid-gas interface approaches and then exceeds the speed of sound in the liquid. A useful definition for transient cavitation can be described by the criterion that R_m must be at least $2.3R_o$, which is the growth needed for the bubble to just reach supersonic collapse velocity (*20*).

The theory also predicts that for a given driving frequency and acoustic pressure P_A, R_m is constant and is independent of the bubble's initial size. Since the size of a bubble determines its stored energy, which may be liberated as kinetic energy during a collapse, the violence of collapse depends on bubble size. Therefore, for frequencies greater than 100 kHz, the violence of a cavitation event will be determined by the driving frequency and the acoustic intensity, decreasing with frequency and increasing with intensity.

The results discussed so far were derived assuming a continuous wave ultrasonic exposure. In a recent new application of Eq. (4), Flynn calculated the cavitation threshold for microsecond acoustic pulses that simulate those used in diagnostic ultrasound (*24*). After partitioning the terms of Eq. (4) into two components, an inertial acceleration function IF, and a pressure acceleration function PF, he plots each one as a function of normalized radius. During the initial stage of collapse, both terms contribute to the bubble's accelerating collapse. Eventually though, the PF term predominates, arresting the motion of the interface. Since Eq. (4) assumes no mass transport, the gas pressure within the bubble cushions its collapse. Thus, the collapse of a vapor-filled bubble will be more violent than the collapse of a gas filled bubble of equal size.

Assuming a single acoustic frequency with a Gaussian envelope to simulate short ultrasonic pulses, Flynn calculates the effect of different initial bubble sizes and driving frequencies for a constant pulse width of 1 μsec. (Since pulse width was constant, the number of cycles per pulse changed with drive frequency.) His results predict that transient cavitation does occur. For example, at 1.0 MHz and a pressure amplitude of 6 bar (with spatial peak temporal peak intensity I_{SPTP} = 24 W/cm^2) (*3*), a nucleus filled with argon with an initial radius of 1.0 μm will expand to a maximum radius of 7.4 μm and then will collapse giving rise to a peak pressure of 28,000 bar and a maximum temperature of 10,000°K.

Using a mathematical definition for cavitation threshold, Flynn calculates threshold values as a function of initial bubble size for several different ultrasonic frequencies. His results are shown in Figure 5. The dashed lines represent regions where the initial bubble size was too large for transient cavitation to occur. Also plotted in this figure is the Blake threshold, which represents the minimum negative static pressure that would cause a bubble to grow without limit. The results in Figure 5

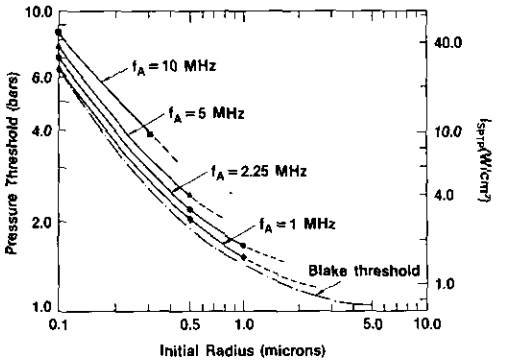

FIGURE 5. Variation of cavitation threshold with initial bubble radius for a constant pulse width of 1.0 μsec.

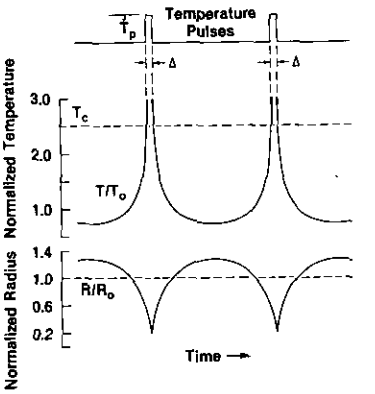

FIGURE 6. Variation of radius and temperature within a bubble oscillating in a sound field. Flashes of light due to sonoluminescence are observed when the bubble's temperature exceeds a critical value, T_c.

show a frequency dependence. The lowest frequency has the lowest threshold, which is just above the Blake threshold. Flynn interprets this result to mean that at 1.0 MHz and below, the effect of a pressure cycle at that frequency on a small nucleus is nearly the same as a static pressure change. Thus, for small nuclei, the Blake threshold is a reliable predictor of the cavitation threshold. Flynn's thresholds are calculated assuming a free (unstable) bubble is present in the liquid. Thresholds that include the effect of nucleation may be considerably higher.

To illustrate how these theoretical predictions successfully explain a variety of experimental results, we will consider one phenomenon associated with transient cavitation, sonoluminescence. Since its discovery in 1933, many explanations have been offered for the origin of this effect. They fall into two broad categories, electrical and thermal. Frenkel proposed that molecular bonds were broken when a new cavity was formed by ultrasound. The charges created formed on opposite walls of the cavity, which was initially lens-shaped. Under certain conditions, microdischarges could occur that produced light (*25*).

Noltingk and Neppiras suggested an alternative, called the "hot spot" theory, in which high intercavity temperatures produced incandescence (*21*). Griffing modified this theory by suggesting that thermal energy produces free radicals that then recombine to produce luminescence (*26*). This idea had the advantage that lower temperatures are required to dissociate water molecules than are required to excite molecules into a radiative state. Frenkel's theory predicts light is emitted during the expansion of the bubble, while the thermal theory predicts it is produced during the bubble's collapse.

Saksena and Nyborg used a cylindrical resonator operating at 30 kHz to study sonoluminescence from bubbles suspended in a viscous mixture of glycerine and water (*27*). The high viscosity of the liquid kept the bubbles from disintegrating upon collapse, providing the investigators with a reproducible means of studying their behavior which they classified as stable cavitation. Surface oscillations would normally cause a bubble in a low viscosity liquid to break into many microbubbles that could later serve as cavitation nuclei.

Saksena and Nyborg observed flashes of light with a period T that was the same as the acoustic period, and a duration that was less than one-tenth of T. These results can be explained by using Figure 6, which is a plot of the normalized radius and temperature within each bubble as a function of time. During each collapse, the bubble's temperature exceeded a critical value T_c that produced light. These results support the hot spot theory that predicts light is emitted during the final stage of a bubble's collapse.

The authors offer two explanations for the light; emission from an ionized gas and emission from the recombination of $^{\cdot}H$ and $^{\cdot}OH$ free radicals. Using thermodynamic considerations, they show the reaction (8):

$$H_2O \rightarrow {}^{\cdot}H + {}^{\cdot}OH \qquad (8)$$

reaches equilibrium in less than 1.0 μsec. at 2000°K, and that the light output from this mechanism is much greater than the light output from the collision of ions with neutral molecules, at least up to 3000°K. When allyl alcohol, a known free radical scavenger which has the same vapor pressure as water, was added to the liquid, no sonoluminescence was observed. This led the authors to conclude that the recombination of $^{\cdot}OH$ and $^{\cdot}H$ radicals is primarily responsible for the light they observed and that the temperature within the bubble exceeds 1800°K.

Young measured the sonoluminescence at 20 kHz for 17 different gases dissolved in water (*28*). He also derived an expression for the temperature of the gas within a collapsing bubble that modifies Eq. (7) to account for thermal conductivity within the gas. The results suggest that different luminous intensities observed in solutions of different gases can be explained by reduced temperatures within a collapsing bubble that are due to the effect of heat conduction within the gas. Similarly, differences in luminous intensity observed for

diatomic gases where $\gamma = 4/3$ and monatomic gases where $\gamma = 5/3$ can be attributed to differences in the temperatures reached during the bubble's collapse (*29*). Thus, in many sonochemical investigations, argon bubbling is used to enhance the effect of cavitation, since argon has a high γ and a low thermal conductivity.

In similar experiments, Verrall et al. observed the light emission from argon-saturated aqueous alkali metal salt solutions sonicated at 460 kHz (*30*). Using spectral broadening of the emission line, which is a consequence of the uncertainty principle, the investigators were able to measure the pressure increases within the collapsing cavities. These results are in agreement with Young's conclusion that adiabatic predictions of final temperatures and pressures of a collapsing bubble are too large but predictions that account for the thermal conductivity of the gas within the cavity are consistent with the experimental data. They also show that the light detected is a gas phase emission since spectra characteristic of mixtures of alkali metal vapor and argon were observed.

The optical spectra of sonoluminescence have also been studied using single-photon counting techniques (*29*). For this experiment, water was saturated with He, Ne, Ar, Kr, O_2, N_2, and air, and the solutions were sonicated at either 330 or 459 kHz. The observed emission spectra are consistent with Griffing's thermal model in which luminescence occurs when ·H and ·OH free radicals recombine. Thus, the results from many different investigators studying sonoluminescence using different experimental techniques suggest that free radicals are produced during transient cavitation events.

Sonoluminescence is spectrally similar to the luminescence of water produced by ionizing or gamma radiation (*29*). For the latter case, hot spots called spurs are generated as previously explained when discussing radiation induced micronuclei. Light is emitted from these spurs either by the emission of excited water molecules which occurs around 260 nm (the mechanism responsible for sonoluminescence) or when excited water molecules decompose to OH^* (Σ^+) and e^- with emission in the regions of 350 nm and 460 nm, respectively. For ionizing radiation, the first emission is called non-Cerenkov, while the second is called Cerenkov. No Cerenkov-like emission was observed during this sonoluminescent spectroscopy study.

Acoustic Methods

In view of the previous discussion, we will now attempt to identify some of the conditions which an investigator must control to obtain reproducible sonochemical results. These broadly fall into three categories: factors that effect the exposure field, the condition of the liquid and the method of observation. For the exposure field, it is necessary to control intensity, frequency, pulse conditions, type of exposure field and total exposure time. Higher intensities lead to larger values of R_m producing higher temperatures during the bubble's collapse and, thus, higher free radical yields. Frequency effects cavitation in at least two ways. As frequency increases, R_m decreases, as does the time available for nucleation and growth. Both factors tend to produce lower free radical yields. Recent investigators have reported cavitation enhancement by pulsed ultrasound for pulse lengths between 6 and 60 μsec, which is explained theoretically by unstabilized nuclei in a critical range that survive from one pulse to the next (*31*).

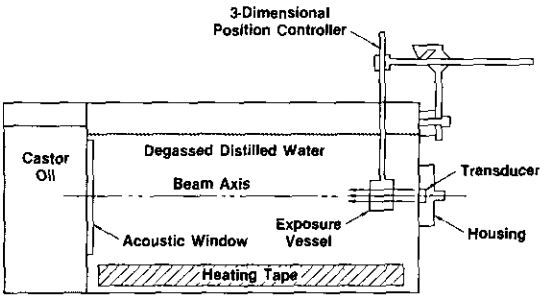

FIGURE 7. Typical free field exposure tank. Castor oil absorbs the ultrasound to minimize standing waves.

Exposure apparatus used for sonochemical studies can be categorized into two types: free field exposure systems and standing wave exposure systems. An example of a free field exposure tank is shown in Figure 7 (*32*). In this particular case, ultrasound at 1.0 MHz is produced at one end of the exposure tank and is absorbed at the other end to minimize standing waves. The size of the exposure vessel is chosen so that it does not interfere with the incident acoustic beam. Acoustically transparent mylar windows are used to seal the test solution in the exposure vessel. Thermoregulation is included. By performing field scans within the tank and calibrating the output of the transducer, it is possible to specify accurately the exposure field [A complete list of parameters needed and their definitions are given elsewhere (*3*).]

In contrast, a typical standing wave exposure tank, in this case designed by Henglein, is shown in Figure 8 (*33*). A transducer operating at 500 kHz is mounted in a rigid assembly that includes an oil bath for cooling. A 100-mL exposure flask is positioned over the transducer with the separation spacing adjusted for maximum acoustic output. The flask is filled with only 30 mL of sample solution. The bottom of the flask is a flat surface 0.2 mm thick to allow good acoustic coupling and heat transfer. Cooling water is provided for temperature regulation. The acoustic beam propagates into the exposure flask and is reflected from the gas liquid interface producing a standing wave within the flask. In a typical application, the acoustic power is intense enough to produce a water spout within the flask (a phenomenon due to radiation force) so that vigorous mechanical mixing also occurs.

This method has some advantages. Because of the standing wave, bubbles less than resonance size are driven to pressure maxima and can grow by rectified

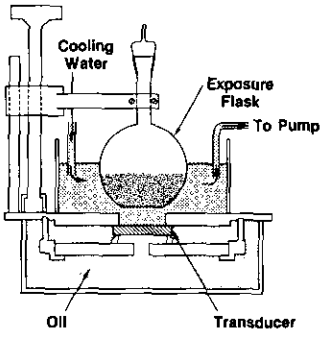

FIGURE 8. Typical standing wave exposure tank. Ultrasound passes through the bottom of the exposure flask and is reflected from the gas liquid interface producing a standing wave.

diffusion. In addition, the mechanical stirring will disperse them throughout the exposure flask. Standing wave systems that trap bubbles and allow them to grow while also providing some stirring appear to be a particularly effective method for enhancing cavitation (*34*). Thus, Henglein's exposure system provides reproducible results.

Its main disadvantage is that the acoustic field within the flask is so complex it is difficult to quantitate. The spatial average intensity I_o at the face of the transducer, usually measured in a free field and the intensity value usually reported, will change in a standing wave field. I_o does not represent the localized maximum acoustic pressure since this quantity will depend on multiple reflections that occur within the flask. Thus, acoustic intensity can usually not be specified. A distinction should be made between this system and resonator systems (*8,9,14*), where standing waves are confined within a specific geometry that results in a well characterized field which can be calibrated.

Another exposure field parameter that must be controlled is total exposure time. Rectified diffusion is particularly effective in degassing a solution. Presumably this explains the results of McKee et al., who found yields of their sonoproducts plateauing with increasing exposure time (*35*). In order to maintain a reasonable reaction rate, air was bubbled through the exposure vessel during insonation. Of course, scattering by these bubbles disturbs the local acoustic field within the exposure vessel, making it difficult to quantitate the exposure field.

Besides controlling exposure parameters, an investigator must also control the condition of his test liquid. Factors that are known to effect the cavitation threshold are gas saturation, type of gas, temperature of the liquid, viscosity, history, surfactant concentration and ionizing radiation level, which may include occasional random effects from natural background radiation. As previously mentioned, the pressure history will effect a liquid's cavitation threshold. We also include in this category any filtering done to remove motes. Apfel estimates ordinary tap water contains as many as 100,000 motes/cm^3 (*11*). Mild filtering appears to have little or no effect on the cavitation threshold (*16*), while protracted filtering has a dramatic effect (*8*). Finally the temperature history of a liquid can be important. Armour and Corry found that cavitation, as measured by cell lysis, was enhanced by storing their specimens at 3°C until gas saturation was achieved and then exposing them at 37°C (*36*). They attributed this effect to supersaturation of the exposed solutions.

Apfel points out that one of the factors that influences cavitation threshold is the method of observation (*2*). At lower frequencies, cavitation events almost always involve multiple bubbles. As the frequency increases, R_m decreases and the violence of the bubble's collapse is less. Therefore, cavitation may occur at higher frequencies but may not be detectible. Part of the increased threshold for cavitation with frequency, observed by Esche (*37*), can be attributed to the difficulty of detecting cavitation at high frequencies. Differences are also expected between the sensitivities of different sonochemical means of detecting free radicals.

Cavitation is a difficult phenomenon to quantitate, requiring over ten parameters to be controlled, as discussed above. Thus, cavitation can be considered to be a measurement of the weakest inhomogeneity present within a liquid at any given time. It is usually observed as a series of random events whose combined effect is often detected when performing sonochemical analyses. Therefore, thresholds only have meaning in the context of a particular experimental set-up and state of the solution exposed. Thus, different thresholds are expected from different investigators. This lack of reproducibility, although expected on theoretical grounds, is, nevertheless, frustrating to the individuals involved, especially since many have experience in the chemistry of ionizing radiation where a given dose produces the same number of free radicals for each exposure. Fortunately, this frustration has not prevented investigators from studying sonochemical effects and reporting them. A review of their results will be presented in the next two sections.

Sonochemistry of Aqueous Solutions

When water containing small gas nuclei is exposed to ultrasound above an intensity threshold, transient cavitation occurs. Within the collapsing cavity very high temperatures and pressures are produced which result in the dissociation of water into hydroxyl radicals and hydrogen atoms. Reactions involving free radicals can occur within the collapsing bubble, at the interface of the bubble, and in the surrounding liquid. A large number of studies of ultrasound-induced reactions in aqueous solutions reported in the 1964 monograph by El'piner (*38*), suggest that chemical changes are brought about by the reactions of hydroxyl radicals and hydrogen atoms.

When water is irradiated with ionizing radiation, the

initial radical species generated are hydrated electrons, hydrogen atoms and hydroxyl radicals, and the initial molecular species formed are hydrogen and hydrogen peroxide (*39,40*). The initial radical species are distributed inhomogeneously in solution and their subsequent behavior has been explained in terms of diffusion kinetics models (*39,40*). Recently, Margulis has investigated the spatial distribution of radicals produced by transient cavitation. Assuming a moderate acoustic field, he shows that individual cavitation events produce local concentrations of radicals which are independent of each · ther. Furthermore, he concludes that cooling occurs more rapidly than diffusion so that only two competing processes need to be considered, recombination or reaction with solutes (*41*). This result is identical to the one obtained in aqueous ionizing radiation chemistry.

For sonochemistry, however, the situation is further complicated by the reactions of radicals in the gas phase, at the gas–liquid boundary and in the liquid phase. In the sonolysis of neutral aqueous solutions hydrated electrons do not appear to be formed. The absence of hydrated electrons in sonochemistry adds support to the belief that Frenkel's charge separation model does not occur and that sonoluminescence is not due to emission from ionized gas.

In aqueous radiation chemistry the primary radical and molecular yields (the number of radicals or molecules produced per 100 eV of ionizing radiation absorbed) $g_{e_{aq}^-}$, g_H, g_{OH}, g_{H_2}, and $g_{H_2O_2}$ can be accurately determined. The g values remain approximately constant over a large range of solute concentration ($\approx 10^{-4} - 10^{-1}$ M).

It seems unlikely that it will be possible to derive an analogous set of g values for aqueous sonochemistry. The formation of ·H and ·OH radicals by ultrasound requires the occurrence of acoustic cavitation. The onset of cavitation is critically dependent on the presence of a population of microbubbles of suitable size, determined by the ultrasound frequency. The bubble population will depend on the nature of the dissolved gases, the history of the liquid, and the number of motes (nonwettable particles containing crevices with undissolved gas). For volatile solutes, in addition to scavenging radicals in the bulk of the solution or in the cavitation bubbles, the temperatures and pressures produced by cavitation may be affected by the changes in the composition and hence the physical properties (vapor pressure, surface tension, thermal conductivity) of the cavitation bubbles.

The chemical effects of ionizing radiation in aqueous solutions depend on pH. Because of the high reactivity of e_{aq}^- with H_3O^+, few hydrated electrons diffuse far from their point of origin in strongly acid solutions. Consequently, the chemistry of acid solutions is largely the chemistry of ·H and ·OH. In strongly alkaline solutions, ·H is converted into e_{aq}^- by reaction with hydroxide ions and ·OH ionizes to ·O^- (*39,40*).

In the sonochemistry of strongly alkaline oxygen-free solutions, the same reactions will occur after diffusion of ·H and ·OH into the bulk of the solutions. Hence, it can be predicted that in the future, reactions typical of hydrated electrons and ·O^- will be characterized in sonochemistry above pH 12.

The similarities between aqueous sonochemistry and radiation chemistry were explored by a number of investigators starting in the early 1950's. A comprehensive account can be found in the 1964 monograph by El'piner (*38*). Some of these studies by Miller in England, Henglein in Germany, Weissler and Anbar and Pecht in the United States will be summarized.

In 1950, Miller (*42*) studied the oxidation of air-saturated ferrous ions (1 mM) in 1N sulfuric acid to ferric ions by 500 kHz ultrasound, a system which is analogous to the classical Fricke dosimeter in radiation chemistry (*39,40*). The ferric ion yield was found to be independent of the ferrous ammonium sulfate concentration above 5×10^{-4} M. Miller concluded that, similar to the effects of ionizing radiation, the oxidative action was an "indirect" process due to the reactive fragments produced in the disruption of water molecules.

The ultrasound induced polymerization of acrylamide in argon and nitrogen saturated aqueous solutions was observed by Henglein in 1952 (*43*). The effects of organic additives on the sonochemical iodine yield from aqueous iodide solutions were also studied (*33*). At low scavenger concentration the behavior of alcohols could be explained in terms of the competition between methanol and iodide ions for hydroxyl radicals.

The effects of varying the ratio of oxygen to that of Kr, Ar, He and N_2 on the sonochemical H_2O_2 yield were examined by Henglein (*44*). At low oxygen concentration (<20%), the H_2O_2 yield increases with oxygen concentration since the recombination reaction:

$$\cdot H + \cdot OH \rightarrow H_2O \tag{9}$$

is suppressed by the reaction

$$\cdot H + O_2 \rightarrow HO_2^{\cdot} \tag{10}$$

which leads to H_2O_2 by

$$HO_2^{\cdot} + HO_2^{\cdot} \rightarrow H_2O_2 + O_2 \tag{11}$$

in addition to that formed by

$$\cdot OH + \cdot OH \rightarrow H_2O_2 \tag{12}$$

Weissler (*45*) investigated the effect of volatile scavengers, acrylamide, formic acid, and allylthiourea on the sonochemical yield of hydrogen peroxide in oxygen and argon saturated aqueous solutions. From these experiments it was inferred that H_2O_2 is formed by the recombination of hydroxyl radicals.

In 1964 Anbar and Pecht (*46*) found that the nonvolatile ·OH scavengers, thallous and formate ions, do not affect the H_2O_2 yields in contrast to volatile organic solutes and concluded that H_2O_2 is not formed by recombination of ·OH radicals in the solution phase.

Anbar and Pecht (*47*) showed that when deuterated formate ions were sonolysed in aqueous solutions, HD

was produced and the yield of HD was independent of solute concentration, indicating that ·H atoms are formed in the sonolysis of water.

More recently, Verrall, Sehgal and Wang, together with other coworkers, have made extensive valuable contributions to sonochemistry. Some of their most significant results will now be discussed. Mead et al. (*48*) investigated aqueous aerated thymine solution and identified four products identical to ones obtained by γ-radiolysis. Their formation could be explained in terms of ·OH and ·H radical reactions. McKee et al. (*35*) studied nucleic acid bases in aqueous solutions under conditions where the ultrasound field could be accurately measured (1 MHz, continuous wave). The order of destruction of the bases was thymine > uracil > cytosine > guanine > adenine. "Threshold" intensities for uracil and thymine were observed at about 0.5 W/cm^2 (SATA). The effectiveness of the dissolved gases in producing sonoreactions was Ar > O_2 > air > N_2 > He > N_2O. Nitrous oxide is well known to convert hydrated electrons to hydroxyl radicals (*39,40*). Since N_2O does not react with ·OH radicals, its large effect on the sonochemical yield appears to be due to an effect on the cavitation process or possibly to its decomposition in the gas phase to nitrogen gas and oxygen atoms.

In another study, Sehgal and Wang (*49*) determined the effects of the bubbling rate on the threshold intensities of thymine destruction. For zero aeration rate, the threshold for thymine reaction was 1.7 W/cm^2 (SATA spatial average temporal average (3). At relatively higher acoustic intensities (> 3W/cm^2) the destruction of thymine was reduced. This was attributed mostly to the change in the number of cavitating bubbles due to an increasing degree of coalescence. The results also suggest that sonoreactions occur at the bubble-liquid interface and the reaction kinetics change with solution temperature. This was explained in terms of opposing changes in cavitation intensity and thymine diffusion as the solution temperature is altered. Figure 9 shows the distribution of concentrations of ·H, ·OH, thymine and reaction products in the neighborhood of a collapsing bubble. The concentration of free radicals is a maximum at the center of the bubble, and decreases in gaussian fashion as one approaches the interphase due to radical recombination (*41*). In the interphase, the radicals react rapidly with thymine resulting in a buildup of the sonoproduct concentration.

Wang and Gupta (*50*) examined the effects of pulsed ultrasound on nucleic acid bases in aqueous solution. Their data suggested that the extent of sonolysis was greater with pulsed ultrasound than with the continuous wave mode at any given temporal average intensity, the extent of sonolysis was greater when the pulse widths were longer within the range studied (20 μsec to 10 msec), and the extent of sonolysis of uracil displayed a maximum at 30% duty cycle, which decreased when the duty cycle was increased or decreased.

Sehgal and Wang (*51*) have used chemical dosimetry to quantify ultrasonically induced transient cavitation. Ferrous and ceric sulfate solutions were used together

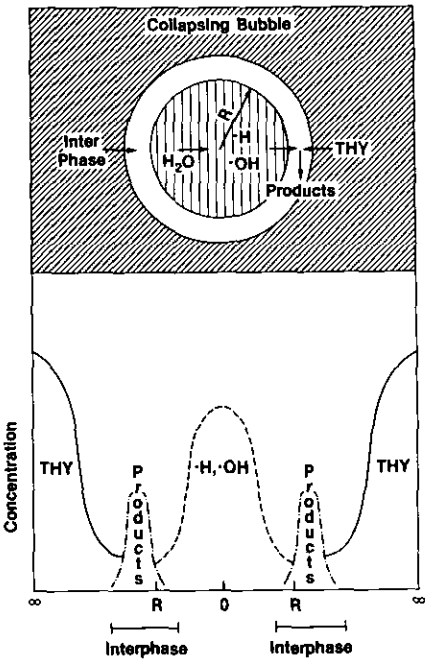

FIGURE 9. Spatial distribution of radical concentration and sonoproducts after transient cavitation event.

to estimate cavitation efficiency (the fraction of the acoustic energy transformed into transient cavitation energy) and chemical efficiency (the fraction of this energy converted into chemical energy). The *G*-values of Fe^{3+} and Ce^{3+} formation were found to be 5.2–5.8 and 2.9 ions per 100 eV of cavitation energy. Oxidation of Fe^{2+} and reduction of Ce^{4+} have been widely used in chemical dosimetry of ionizing radiation. The *G*-values have been measured as a function of linear energy transfer (LET) (LET is defined as the energy transferred per unit length of track, eV/Å). $G(Ce^{3+})$ is almost independent of LET, while $G(Fe^{3+})$ in oxygenated solutions decreases for LET higher than 0.1 eV/Å and approaches an asymptotic value of 3 for heavy fission products. The ratio $M = G(Fe^{3+})/G(Ce^{4+}) = 1.8–2.0$ corresponds to ionizing radiation of LET 8–9 eV/Å. This value of *M* is in good agreement with the results of Weissler (*52*). Hence, ultrasonic cavitation in oxygen saturated solutions is analogous in certain respects to the action of α-particles from ^{210}Po (LET = 8.8 eV/Å) and differs from fission radiation as predicted by Margulis on the basis of a diffusion model (*41*).

Spin Trapping and ESR Studies

By means of spin trapping and ESR, conclusive evidence for the formation of ·OH radicals and ·H atoms by sonolysis of aqueous solutions has been obtained (*53,54*). In spin trapping (*55–59*), a diamagnetic nitrone or nitroso compound (the spin trap) is used to convert the short-lived radicals into relatively longer-lived nitroxide radicals (the spin adduct) observable by conventional ESR. In an application of spin trapping to

sonochemistry (*60*), it was shown that free radicals produced by the sonolysis of carbon tetrachloride, but not of aqueous solutions, can be spin trapped by 2-methyl-2-nitrosopropane (MNP) and identified by ESR.

To detect the hydrogen atoms and hydroxyl radicals produced by ultrasound, the non-volatile nitrone spin traps DMPO (5,5-dimethylpyrroline-N-oxide), 4-POBN (α-4-pyridyl-1-oxide *N-tert*-butylnitrone), and 4-PYBN (α-4-*N*-methylpyridinium-*N-tert*-butylnitrone) were used. The reactions of the three nitrones with the radical R· (where R· is OH, H, D, or a radical produced by the reaction of one of these species with added scavengers such as formate or ethanol) are shown below:

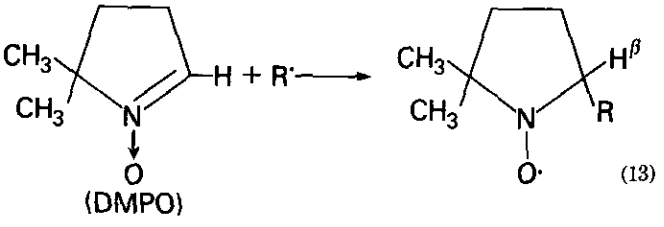

(13)

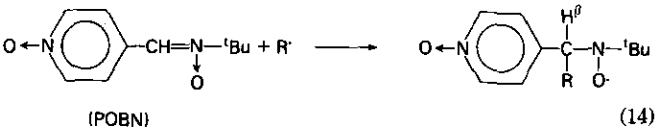

(14)

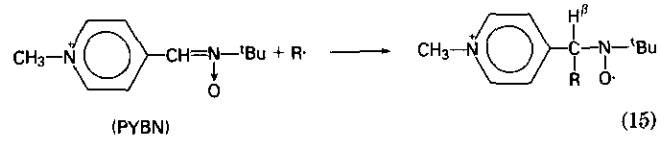

(15)

It should be noted that reactions (13) – (15) are not the only pathways by which hydroxyl radicals and hydrogen atoms react with the nitrone spin traps. Recently, it has been shown that in γ-irradiated aqueous solutions, where the yields of ·OH and ·H are accurately known, only 35% of ·OH radicals react with DMPO, as shown in Eq. (13), and only 14% of ·H atoms react with 4-POBN, as shown in reaction (14) (*61*). These spin-trapping efficiencies were obtained under conditions where the spin-trap concentration is in the "plateau region" in a plot of spin adduct yield versus spin trap concentration, where ·OH radical recombination and spin adduct decay can be neglected. The low spin trapping efficiency of DMPO may be explained by the reactions of ·OH radicals to abstract hydrogen from the DMPO molecule to produce carbon radicals. For 4-POBN, the low spin trapping efficiency for ·H atoms is explained in terms of addition reactions of hydrogen atoms to the aromatic ring and the pyridinium and nitrone oxygens. In a pulse radiolysis study, it has been shown that 40% of the hydroxyl radicals react with 4–POBN to form the ESR detectable nitroxide radical while 60% react with the pyridine ring (*62*).

In the initial studies (*53,54*), the aqueous solutions containing nitrone spin traps were sonicated in a Bransonic 12 ultrasonic bath (50 kHz) at room temperature with argon gas bubbling at a flow rate of 0.5 L/min. The ESR spectra of the sonicated solutions were measured

Table 1. Hyperfine coupling constants of spin-trapped radicals.

Spin trap	Untrapped Radical	Coupling constant, G			
		a_N	a_H^β	a_D^β	a_H^γ
DMPO	·OH	14.9	14.9		
	·H	16.6	22.5		
	·D	16.6	22.5	3.4	
	·COO⁻	15.6	18.7		
	$CH_3\dot{C}HOH$	15.8	22.8		
PYBN	·OH	14.7	1.5		0.4
	·H	16.0	10.0		
	·D	16.0	10.0	1.5	
POBN	·H	16.2	10.2		
	·D	16.2	10.2	1.5	
	·COO⁻	15.5	3.0		
	$CH_3\dot{C}HOH$	15.5	2.6		

in an aqueous quartz flat cell (60 × 10 × 0.25 mm) with a Varian E-9 spectrometer (X band, 100-kHz field modulation). The hydroxyl radicals and hydrogen atoms generated by sonolysis were spin trapped with DMPO or PYBN and the observed spin adducts DMPO-OH, DMPO-H, PYBN-OH, and PYBN-H were identified by comparison with the known literature values of the hyperfine coupling constants. For POBN only, the POBN-H adduct could be detected since the lifetime of the POBN-OH adduct is too short to be observable in these experiments (*54*). Analogous experiments on the sonolysis of D_2O solutions led to the formation of characteristic D spin adducts of DMPO, 4-PYBN and 4-POBN. The hyperfine coupling constants of the spin trapped radicals are shown in Table 1.

The ESR spectra of the DMPO-OH, DMPO-H, and DMPO-D spin adducts obtained from sonolyzed argon-saturated aqueous DPMO solutions are shown in Figure 10*a* and Figure 10*e*, respectively. The effects of adding increasing concentrations of ethanol are illustrated in Figures 10*b*, 10*c*, and 10*d*.

It has been reported that there are three other pathways that produce OH and H spin adducts which do not depend on the formation of hydroxyl radicals and hydrogen atoms. First, DMPO can be converted into the isomeric oxazirane by photochemical rearrangement or by reaction with H_2O_2 (*63*), as shown in Eq. (16).

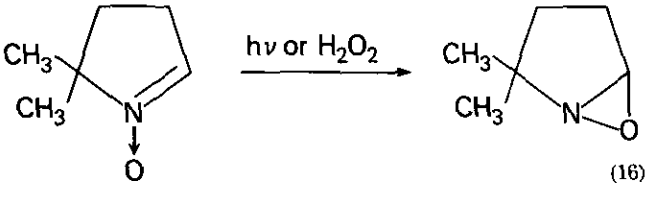

(16)

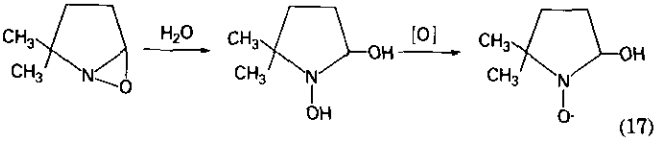

(17)

The hydrolysis of the epoxy ring shown in Eq. (17) leads

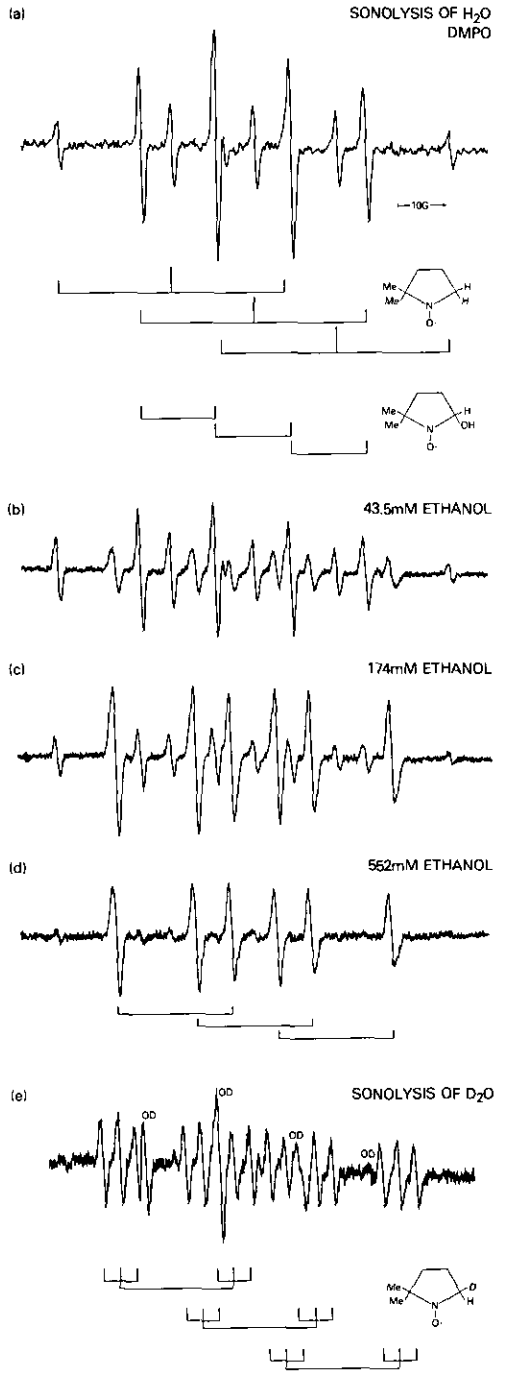

FIGURE 10. ESR spectra of spin-trapped radicals obtained by sonolysis (3 min.) from aqueous solutions containing DMPO (75 mM) and ethanol: (*a*) none; (*b*) 43.5 mM; (*c*) 174 mM; (*d*) 552 mM; (*e*) a D_2O solution containing DMPO (1 mM). Spectrometer settings are as follows: modulation amplitude, 0.63 G; receiver gain, 4.0×10^4 for (*a*), 6.3×10^4 for (*b*), (*c*), and (*d*), 2.0×10^5 for (*e*); time constant, 0.5 sec for (*a*), (*b*), (*c*), and (*d*), 1 sec for (*e*); scan time, 8 min for (*a*), 30 min for (*b*), (*c*), and (*d*), and 1 hr for (*e*).

to the production of the hydroxylamine which is oxidized to form the same nitroxide radical as obtained by spin trapping of $^{\cdot}OH$ with DMPO. Second, the hydroxyl adduct of POBN can be produced by the acid catalyzed addition of water followed by H_2O_2 addition (*64*). Since H_2O_2 is formed by sonolysis of water, it is conceivable that the PYBN-OH adduct could be produced by such a pathway. Third, the hydrogen adducts of all three spin traps could be formed by the reaction of the hydrated electron (e_{aq}^-) with the spin traps, followed by protonation (*65*).

Direct formation of $^{\cdot}OH$ and $^{\cdot}H$ from water by sonolysis rather than by these other pathways was verified by carrying out other experiments in which scavengers compete with spin traps, DMPO and POBN for $^{\cdot}OH$ and $^{\cdot}H$. When aqueous DMPO solutions containing various concentrations of scavengers (ethanol, sodium formate) were sonicated, a decrease in the signal intensity of the DMPO-OH adduct and a corresponding increase of the DMPO–CO_2^- and DMPO–C_2H_4OH adducts was observed as the scavenger concentration was increased at constant DMPO concentration. These changes indicate that competitive scavenging of $^{\cdot}OH$ by DMPO has occurred since the changes in the ESR spectra take place when the products of the reaction rate k and the scavenger concentration [S], $k_{S+\ OH}[S]$ *is comparable to* $k_{DMPO+\ OH}[DMPO]$.

The effect of increasing ethanol concentrations in decreasing the POBN-H spin adduct formed by sonolysis clearly indicates that the $^{\cdot}H$ adduct is not formed by the reaction of hydrated electrons with POBN followed by proton transfer. Alcohols are essentially unreactive with hydrated electrons. The rate constant for the reaction of hydrated electrons with ethanol at room temperature is $k_{e^-_{aq}\ +\ EtOH} < 4 \times 10^2$ L/moles–sec (*40*).

The effects of a variety of $^{\cdot}OH$ radical scavengers on 440 the DMPO-OH yield produced by sonolysis in argon-bubbled and air-saturated solutions have been studied. In argon-bubbled solutions, the scavengers were formate, thiocyanate, methanol and 2-methyl-2-propanol while in air-saturated solutions, formate, ethanol, acetone and 2-methyl-2-nitrosopropane (MNP) were investigated. The ESR intensity of the DMPO-OH adducts decreases as a function of $k_{S\ +\ OH}[S]$ above a threshold, where [S] is the concentration of the scavenger in the bulk of the solution. For radical competition reactions in homogeneous solution, the data for all scavengers would be expected to fit on a single curve. However, acetone and MNP react with $^{\cdot}OH$ as if their effective *rate constants were two orders of magnitude greater* than the known values for acetone and MNP in aqueous solutions. The unusual effects of acetone and MNP indicate that $^{\cdot}OH$ radicals are produced in the collapse of transient cavitation bubbles. It has been reported that MNP could not spin trap free radicals in sonolysed solutions containing amino acids, dipeptides and DNA bases except the *tert*-butyl radical (*60*). This suggests the possibility that MNP reacts with $^{\cdot}H$ and $^{\cdot}OH$ in the cavitation bubbles so that these radicals cannot diffuse into the bulk of the solution to react with other solutes. Since the $^{\cdot}OH$ and $^{\cdot}H$ adducts of MNP are known to be very unstable (*55*), this could explain the failure to spin trap organic radicals in aqueous solutions containing

MNP as the spin trap. Alternatively, MNP and acetone may affect the high temperatures and pressures produced by transient cavitation and, thus, reduce the yield of hydroxyl radicals.

Similar studies of the effect of ·H atom scavenger concentration on the POBN-H spin adduct yield produced by sonolysis were also carried out. The results were analogous to those obtained for the ·OH radical scavengers.

Hydroxyl radicals and hydrogen atoms have also been observed in argon-saturated aqueous solutions exposed to ultrasound (25 kHz) by using clinical dental equipment (*66*).

In order to carry out spin trapping experiments under conditions were the acoustic exposure field can be measured accurately, experiments were carried out in a special exposure apparatus (*32,67*). For continuous-wave 1 MHz ultrasound, the intensity threshold for radical production was 0.7 W/cm^2 spatial peak temporal average (SPTA). The yields of ·OH radicals varied; however, when a response was recorded, the yields were linear as a function of intensity and the plots intersected at a common threshold. Competition studies with formate and ethanol in argon-saturated solutions indicated that the DMPO-OH and POBN-H spin adducts were generated from ·OH radicals and ·H atoms.

Recent theoretical calculations by Flynn (*24*), have shown that small gas nuclei in water exposed to microsecond pulses above an intensity threshold may grow into transient cavities that collapse violently. Aqueous solutions were studied over a range of pulse widths from 1 msec to 6.5 μsec and pulse repitition frequencies from 0.5 – 100 kHz at a spatial average temporal average (SATA) intensity of 1.5 W/cm^2. Even for the case of 6.5 μsec and 4 kHz, a significant radical yield was observed at an intensity of 2.4 W/cm^2 (SPTA) and 140 W/cm^2 temporal maximum. These results indicate that in aqueous solution transient cavitation and free radical formation occur under simulated diagnostic conditions. For these simulated diagnostic pulses, the number of ·OH radicals spin trapped per 6.5 μsec pulse was in the range from 10^7 to 10^8 radicals/mL; for 1 msec pulses, 10^{10} ·OH radicals/mL were observed. For comparison, 1 mrad of Co gamma radiation generates 1.7×10^9 ·OH radicals/mL in aqueous solutions.

Edmonds and Sancier (*68*) have studied free-radical production in media of viscosity and surface tension equivalent to mammalian body fluids and tissue. Argon-saturated solutions containing DMPO as the spin trap were rotated at 30 rpm at 4 – 8°C in a 1 MHz ultrasound facility where dosimetry could be performed accurately. Trypsin solutions, Dulbecco's Minimum Essential Medium, fetal bovine serum, human blood plasma and whole human blood were investigated. Exposure to continuous wave ultrasound at 6.6 W/cm^2 (SPTA) for 15 min in the presence of 10 mM DMPO results in the formation of DMPO-OH and DMPO-H spin adducts even in the presence of natural radical scavengers in the mammalian-derived products.

Recently, Rehorek and Janzen (*69*) have applied spin-trapping to the study of free radicals produced by ultrasonic decomposition of organometallic compounds. Nitrogen-saturated aqueous solutions containing $[Co(NH_3)_5N_3]Cl_2$ and DMPO were exposed to ultrasound in a Bransonic 220 cleaning bath (55 kHz) at room temperature. The effects of varying the concentration of the Co complex and of DMPO were investigated. Spin adducts of the azide radical ($N^{\cdot}_3$), as well as smaller amounts of DMPO-OH and traces of DMPO-H, were identified. The results were consistent with the mechanism shown in Eqs. (18)–(20).

$$H_2O \rightarrow {}^{\cdot}H + {}^{\cdot}OH \tag{18}$$

$${}^{\cdot}H + [Co(NH_3)_5N_3]^{2+} \rightarrow Co^{2+} + NH_4^+ + 4NH_3 + N_3^- \tag{19}$$

$${}^{\cdot}OH + N_3^- \rightarrow OH^- + {}^{\cdot}N_3 \tag{20}$$

Increasing the spin trap concentration from 10^{-3} M to 0.2 M resulted in a decreasing signal intensity of the azide spin adduct and an increase in the DMPO-OH and DMPO-H signals. An increase of the Co (III) complex concentration led to a decrease of the DMPO-H signal and finally to its disappearance.

Sonochemistry of Nonaqueous Solutions

In aqueous solutions, the major mechanism of chemical action resulting from cavitation is the dissociation of water into hydrogen atoms and hydroxyl radicals and the subsequent reaction of these intermediates. The failure to observe in organic media certain sonochemical reactions which occur readily in water led some early investigators to conclude that the high vapor pressures of non-aqueous solvents render them incapable of sustaining cavitationally induced reactions (*38,70*). Supporting this view was the observation that aqueous sonochemical reactions could be suppressed by the addition of small amounts of organic solvents. It has become increasingly apparent that cavitation can and does occur in organic solvents (*71*), and, although it is generally less intense than in water, can have profound effects on chemical transformations and on the medium itself. A systematic study of the effect of cavitation on organic liquids is lacking, but is becoming an area of interest and importance as ultrasound is used more frequently as a tool in synthesis.

This review will provide examples of free radical formation in organic liquids under the influence of high intensity ultrasound in three major areas. These include cavitation induced decomposition of solvent or solute, ultrasonically initiated free radical polymerization (closely related to the former), and ultrasonic polymer degradation. An area which will not be included deals with ultrasonically promoted reactions in which free radical intermediates are produced chemically subsequent to the cavitation event. The use of ultrasound in the formation of Grignard and other organometallic reagents (*72*), and in the alkali metal mediated coupling

of acyl, aryl (*73*), or silyl (*74*) halides fits this latter category since the intermediate free radicals are not the direct result of a cavitational event, but instead are produced by dissociative electron transfer from an active metal. The rate enhancements in these reactions are generally thought to be the consequence of ultrasonic cleaning of the reactive metal surface.

Three techniques of varying sophistication and reliability have been used to decide whether free radicals are formed on exposure of organic liquids to ultrasonic waves. These include product studies, chemical probes (initiation of polymerization, reaction with stable free radicals, etc.), and spin trapping and electron spin resonance (ESR) analysis. The number of studies is few enough that the topic can be approached on nearly a compound by compound basis.

Schultz and Henglein (*75*) used two chemical probes in their study of the effect of ultrasound on methanol. They sonicated anhydrous methanol containing the stable radical 2,2-diphenyl-1-picrylhydrazyl (DPPH) and observed bleaching characteristic of the reaction of this compound with radicals. In addition, they found that the radical chain polymerization of acrylamide could be initiated by the free radicals generated ultrasonically, and suggest that their formation may occur by the dissociation of methanol in a manner analogous to water. The identities of the radicals produced remain to be established. Spin trapping and ESR experiments which have allowed spectroscopic identification of radicals in many radiolysis and other sonolysis studies have not been reported in the case of methanol.

In other early work, Weissler et al. (*76*) analyzed volatile products resulting from the ultrasonic decomposition of acetonitrile and carbon tetrachloride. The products [Eqs. (21) – (24)] clearly indicate the free-radical nature of the reactions. Further evidence was obtained by varying the atmospheres under which the experiments were performed. When acetonitrile was irradiated in a mixture of D_2 and Ar, comparable yields of HD and H_2 were formed indicating that hydrogen atoms were a primary product. The rate of chlorine production from CCl_4 under Ar was observed to be slower than when the reaction was under oxygen. However, when *n*-butyl iodide was added to suppress the back reaction of $\cdot CCl_3$, the rate under argon rose to 8×10^{-7} mole/L – min. Direct spectroscopic evidence for free radical formation in the sonication of CCl_4 (and CCl_3Br) has been provided by Rosenthal et al. (*60*). When either liquid was sonicated in the presence of 2-methyl-2-nitrosopropane as the spin trap and analyzed by ESR, a spectrum characteristic of an acyl spin adduct was obtained [Eqs. (25) and (26)].

$$CH_3CN \text{ (argon)} \rightarrow N_2 + CH_4 + H_2O \quad (21)$$

$$CH_3CN \text{ (oxygen)} \rightarrow N_2 + CO + CO_2 + H_2O \quad (22)$$

$$CCl_4 \text{ (oxygen)} \rightarrow Cl_2$$
$$k = 5 \times 10^{-7} \text{ mole/L-min} \quad (23)$$

$$CCl_4 \text{ (argon)} \rightarrow Cl_2$$
$$k = 1 \times 10^{-8} \text{ mole/L-min} \quad (24)$$

$$CCl_4 \xrightarrow{)))} CCl_3^{\cdot} + X^{\cdot} \quad (25)$$

$$CCl_3^{\cdot} + tBu-N=O \rightarrow Cl-\overset{\overset{O}{\|}}{C}-\underset{\underset{O^{\cdot}}{|}}{N}-tBu \quad (26)$$

The adduct was produced in either air or nitrogen flushed solution, as well as in solutions that were carefully degassed, indicating that its oxygen atom originates in the spin trap. A mechanism for its formation has been proposed based on that suggested for its photochemical generation.

Chloroform has also been subjected to ultrasonic degradation (A. Henglein, personal communication). The products [Eqs. (27) and (28)] appear to result from both radical and carbene intermediates. Sonolysis in the presence of cyclohexene as a chemical probe led to formation of 7,7-dichloro-bicyclo [4.1.0] heptane and cyclohexyl chloride in addition to other products. The former is taken as good evidence for dichlorocarbene formation, and the latter for radical addition to a double bond. Suslick and Schubert (*77*) found evidence for ultrasonic degradation of chloroform in their studies on the sonochemistry of $Mn_2(CO)_{10}$ and $Re_2(CO)_{10}$. Whereas $Re_2(CO)_{10}$ is inert to ligand exchange (with phosphines) in hydrocarbon solvents, both $Re_2(CO)_{10}$ and $Mn_2(CO)_{10}$ undergo rapid chlorination when sonicated in chloroform and a variety of other halocarbons. The rate of reaction is independent of the concentration of $M_2(CO)_{10}$ so the rate limiting step does not involve the metal carbonyl. Halogenation is suppressed when hydrocarbon-halocarbon mixtures are used as solvents. The products in this case are halogenated hydrocarbons and HX resulting from trapping of $X^{\cdot}$ by the alkane. A free radical mechanism based on the sonochemical cleavage of the chlorocarbon solvent was proposed to account for the observation [Eqs. (29)–(33)].

Suslick et al. (*78*) found that even alkanes are subject to sonolysis and that the reaction shows remarkable similarities to high temperature pyrolysis (1200° C). The products are consistent with the operation of a Rice radical-chain mechanism [Eqs. (34)–(43)]. The use of diphenylpicrylhydrazyl as a chemical probe completely inhibited the formation of products and the rate of decomposition was found to be inversely proportional to the vapor pressure.

$$CHCl_3 \xrightarrow{))))} \begin{matrix} H_2,\ HCl,\ CH_2Cl_2,\ CCl_4,\ C_2Cl_6 \\ C_2HCl_5,\ C_2H_2Cl_4,\ C_2H_2Cl_2, \\ C_2HCl_3,\ C_2Cl_4 \end{matrix} \quad (27)$$

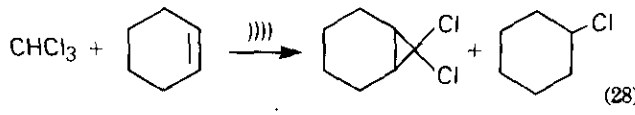

(28)

$$R_3CX \xrightarrow{)))} R_3C^{\cdot} + X^{\cdot} \quad (29)$$

$$2R_3C^{\cdot} \rightarrow R_3CCR_3 \quad (30)$$

$$2X^{\cdot} \rightarrow X_2 \quad (31)$$

$$M_2(CO)_{10} + 2X^{\cdot} \rightarrow 2M(CO)_5X \quad (32)$$

$$M_2(CO)_{10} + X_2 \rightarrow 2M(CO)_5X \quad (33)$$

$$C_{10}H_{22} \xrightarrow{)))} H_2,\ CH_4,\ C_2H_2,\ C_2H_4,\ C_2H_6,\ C_3H_4,\ C_3H_6,\ C_3H_8,\ 1\text{-}C_4H_8,\ C_4H_{10},\ 1\text{-}C_5H_{10},\ C_5H_{12},\ 1\text{-}C_6H_{12},\ C_6H_{14},\ 1\text{-}C_7H_{14},\ C_7H_{16},\ 1\text{-}C_8H_{16},\ C_8H_{18},\ 1\text{-}C_9H_{18},\ C_9H_{20} \quad (34)$$

$$C_{10}H_{22} \rightarrow 2R^{\cdot} \quad (35)$$

$$R^{\cdot} \rightarrow R^{\cdot} + C_2H_4 \quad (36)$$

$$R^{\cdot} \rightarrow R - CH_2 - CH{=}CH_2 + H^{\cdot} \quad (37)$$

$$R^{\cdot} + C_{10}H_{22} \rightarrow RH + R\overset{\cdot}{\wedge}R \quad (38)$$

$$H^{\cdot} + C_{10}H_{22} \rightarrow H_2 + R\overset{\cdot}{\wedge}R \quad (39)$$

$$R\overset{\cdot}{\wedge}R \rightarrow R - CH_2 - CH{=}CH_2 + R^{\cdot} \quad (40)$$

$$R^{\cdot} + R^{\cdot} \rightarrow R - R \quad (41)$$

$$R^{\cdot} + H^{\cdot} \rightarrow R - H \quad (42)$$

$$H^{\cdot} + H^{\cdot} \rightarrow H_2 \quad (43)$$

By combining the use of two dosimeters, $Fe(CO)_5$ (*79,80*) and DPPH, Suslick and co-workers (*81,82*) have evaluated the effectiveness of various solvents in producing cavitational sonochemistry in general and free radical formation in particular. The influence of solvent properties are quite complex and remain to be entirely sorted out. In addition to solvent vapor pressure, viscosity and bond dissociation energy have significant importance. Suslick's conclusion is that solvent vapor pressure is the most important contributor. Within a given class of compounds (for example, alkanes, alcohols, etc.) very good correlation exists between the log of the rate of a sonochemical reaction (unique decomposition of $Fe(CO)_5$ or bleaching of DPPH) and the solvent vapor pressure. The higher the vapor pressure the slower the reaction rate, which leads, incidentally, to the curious phenomenon of an inverse relationship between macroscopic temperature and rate in these sonochemical reactions. A much weaker correlation is observed when comparing liquids of different classes, as bond dissociation energy becomes more significant. Thus, a list of solvents (*82*) in decreasing order of radical forming ability as measured by DPPH bleaching shows the complex nature of the problem (Table 2). Solvent vapor pressure significantly influences the intensity of the cavitational collapse and, therefore, the temperataure and pressure achieved in the vicinity of the cavitation bubble and ultimately, the rate of sonochemical reactions.

Table 2. Rate of DPPH trapping in nonaqueous solvents.

Solvent	Vapor pressure, torr	$-d$[DPPH]/dt μM/min
Decalin	0.20	11.8
Mesitylene	0.53	11.4
Di-*n*-butyl ether	1.9	10.4
Cyclohexanone	1.3	8.91
Decane	0.25	7.75
1-Hexanol	0.12	7.74
m-Xylene	2.2	7.25
1-Pentanol	0.35	6.66
1-Butanol	1.1	6.20
2-Hexanone	10.1	5.44
1-Propanol	4.6	5.43
2-Pentanone	11.3	4.13
Toluene	8.7	2.17
Di-*n*-propyl ether	22.8	1.61

Solutes in organic solution have also been found to undergo sonolytic reactions. The effect of ultrasound on a series of organotin compounds has been studied by Rehorek and Janzen (*83*). Carbon-centered radicals were trapped using nitrosodurene and the mixture of aminoxyl radicals were identified by ESR [Eqs. (44) and (45)]. Evidence for tin-centered radicals, which do not couple with nitrosodurene, was obtained by sonication in the presence of alkyl iodides. Alkyl-durylaminoxyls were obtained in these cases from the alkyl radicals generated from reaction of the tin radicals with the iodides.

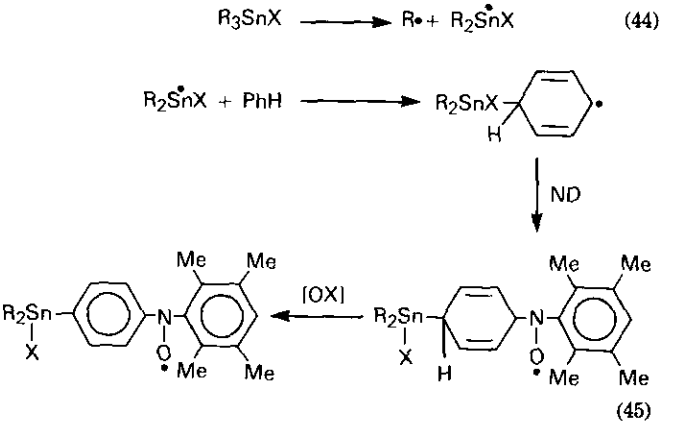

(44)

(45)

A very unusual and somewhat puzzling example of the beneficial use of ultrasound in organic synthesis was reported by Toy and Stringham (*84*). Although the free radical addition of dimethyl disulfide to hexafluoro-2-butyne occurs readily upon photolysis, dimethyl disulfide could be added to hexafluorobutadiene only when irradiated with both UV light and ultrasound. Used

singly, UV or ultrasonic irradiation failed to produce any products. It was suggested that ultrasound serves to homogenize the immiscible reactants allowing photolytic initiation of the presumed free radical mechanism [Eqs. (46) – (48)].

$$CH_3SSCH_3 \xrightarrow[h\nu]{))))} 2CH_3S^{\cdot} \quad (46)$$

$$CH_3S^{\cdot} + CF_2{=}CFCF{=}CF_2 \rightarrow CH_3SCF_2\dot{C}FCF{=}CF_2 \quad (47)$$

$$CH_3SCF_2\dot{C}FCF{=}CF_2 + CH_3S^{\cdot} \rightarrow CH_3SCF_2CF{=}CFCF_2SCH_3 \quad (48)$$

The radicals formed on ultrasonic irradiation of many unsaturated organic molecules can initiate polymerization of the material. In three papers, Kruus and coworkers (*85–87*) studied the polymerization of a variety of aromatic and olefinic materials under the influence of ultrasound. They obtained polymeric charlike residues on exposure of substituted benzenes to ultrasound intensive enough to cause cavitation. Unfortunately, these materials can not be easily characterized, and the only analytical tool used to determine their structure has been elemental analysis. The solid residues gave, however, large broad ESR signals and were thought to result from a radical polymerization mechanism similar to that observed in radiolysis. Rates of darkening (assumed to be related to the polymerization process) were measured by UV for benzene, toluene, chlorobenzene, bromobenzene, iodobenzene, aniline, nitrobenzene, acetophenone, and anisole and the authors noted a rough correlation between bond dissociation energy and reaction rate.

More typical monomers have been studied as well. Although irradiation of acrylonitrile reportedly gave a charlike residue (*85*), styrene and methyl methacrylate underwent typical free radical chain polymerization. In the case of polystyrene, lower molecular weights were obtained from ultrasound-initiated than from thermally initiated polymerization (*88*). In addition, the radical ultrasonic copolymerization of styrene and methyl methacrylate has been studied in the presence of aluminum acetylacetonate as initiator (*89*).

Ultrasonic polymer degradation has been the subject of considerable research and an excellent review article has been published (*5*). In this review, only those papers directly related to the formation of radicals in organic media will be discussed. The ultrasonic degradation of a polymer in solution is a nonrandom mechanical process resulting from hydrodynamic processes arising from cavitation. Polymer chains cleave perferentially near their centers, higher molecular weight fractions degrade faster than ones of lower molecular weight, and a lower molecular weight limit exists below which no further degradation occurs.

For a variety of polymers, homolytic reactions leading to the formation of macroradicals have been postulated to occur. Henglein has reported the use of DPPH (*90,91*) and iodine (*92*) to detect free radical fragments produced in the ultrasonic decomposition of poly (methyl methacrylate). He observed that in the absence of oxygen two molecules of DPPH (or atoms of iodine) are consumed per ruptured C-C bond. In addition, he has studied the recombination of macroradicals from poly (methyl methacrylate) and polystyrene.

The free radicals formed on depolymerization have been used as initiators of chain polymerization reactions (*91*), and by this method, block co-polymers of various types have been produced (*93–95*). Block copolymers have also been prepared by irradiation of mixtures of two homopolymers (*91,96,97*).

Direct evidence for the formation of macroradicals in the ultrasonic degradation of poly(methyl methacrylate), polystyrene and poly(vinyl acetate) has been provided by Tabata et al. (*98,99*) using spin trapping and ESR techniques. They observed ESR spectra of the two spin adducts resulting from a pair of radicals formed by main chain homolysis of these polymers [Eq. (49)]. The formation of other possible radical species was ruled out by ESR studies using polymers selectively labeled with deuterium and observing again only those spin adducts arising from scission of the polymer backbone. These experiments completely eliminate the possibility that polymer degradation might occur by secondary reactions initiated by ions or radicals produced by the action of ultrasound on the solvent. Instead, the macroradicals result from the effect of ultrasonically induced hydrodynamic action on the polymer itself.

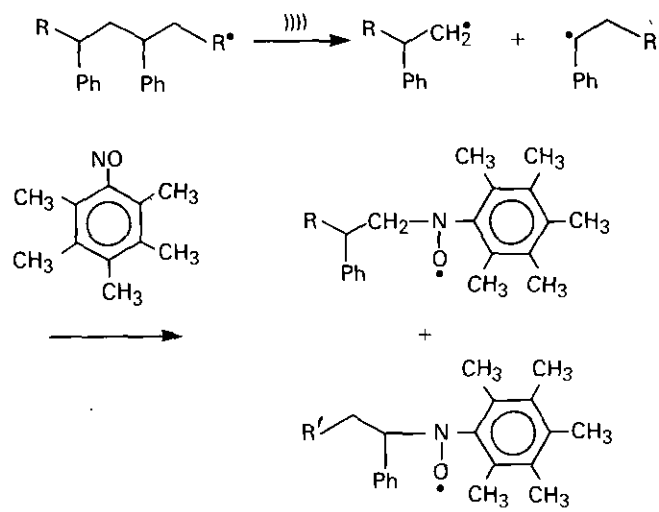

Public Health Implications

Investigations of free radicals generated by ultrasound have public health implications primarily because

they are used to assess the risk associated with the medical use of ultrasound. Although *in vivo* free radical production by ultrasonic cavitation has not been established, this mechanism for inducing biological effects cannot prudently be excluded, especially considering the known biological consequences of free radical production.

It is generally accepted that hydroxyl radicals are responsible for the reproductive death of mammalian cells exposed to ionizing radiation (*100*). Roots and Okada (*101–102*) and Chapman (*103*) have obtained evidence to indicate that $^{\cdot}OH$ radicals rather than hydrogen atoms and hydrated electrons are the species mainly responsible for the indirect effect of radiation injury measured by DNA single strand breaks or cell killing. In the presence of oxygen, $^{\cdot}H$ atoms are converted to $HO_2^{\cdot}$ radicals which are the acid form of superoxide anion radicals ($pK = 4.8$). These radicals can reduce ferric and cupric ions bound to biologically important macromolecules and, thus, lead to site-specific generation of hydroxyl radicals via the Fenton reaction between hydrogen peroxide and reduced transition metal ions. (*104*).

Any detrimental biological consequences of ultrasonic exposure, even assuming a low frequency of occurrence, would have important public health implications because of the wide use of ultrasound in the clinical practice of medicine. Johnson and Abernathy estimate that over 7 million ultrasonic diagnostic imaging procedures were performed in the United States in 1980, compared to 140 million plain film radiographic procedures in the same year (*105*). Of these, 44% were for obstetrical/gynecological applications, 29% were for abdominal scans, and 21% were for echocardiographic applications.

Most of these procedures were performed using B-scan ultrasonic imaging devices. Although the spatial average intensity of these pulse-echo devices is typically low, their spatial peak intensities can be enormous. Carson measured the output from a few commercially available scanners and found the highest spatial peak temporal peak intensity to be 1700 W/cm^2 (*106*). Even accounting for tissue attenuation, the maximum intensity generated *in vivo* for some ultrasonic imaging devices will be in the range of several hundred watts per square centimeter. Since the purpose of a diagnostic imaging procedure is to provide information, these high intensities raise concern over the possibility that some undesirable biological effects may also occur.

One mechanism, by which deleterious effects could occur, is through the action of free radicals formed during ultrasonically generated cavitation. A single bubble has the potential to liberate enormous numbers of free radicals. Apfel has shown that a bubble which has grown substantially to a radius of 5 μm has a potential energy of about 300 MeV (*107*). If the bubble is vapor-filled, then most of this potential energy can be converted to kinetic energy during its subsequent collapse. Cavitation produced by microsecond pulses, typical of ultrasonic imaging devices, was until recently considered unlikely (*108*). New theoretical (*24*) and experimental studies (*67*) have shown that simulated diagnostic microsecond pulses can produce acoustic cavitation in aqueous solutions as observed by the formation of free radicals.

These results are interesting, but do not prove that free radicals are generated *in vivo* by ultrasonic exposure. It is generally accepted that for cavitation to occur *in vivo* at the intensities produced by diagnostic devices, certain unspecified inhomogeneities must exist within the biological system to act as cavitation nuclei.

Conflicting evidence provides little insight into the extent of their existence *in vivo*. Perhaps, the best evidence for cavitation nuclei in tissue is an experiment performed by ter Haar and Daniels (*109*). In this experiment, the hind limb of a guinea pig was exposed to four different levels of ultrasound at 0.75 MHz, simulating therapeutic treatments. Bubbles were observed using an ultrasonic imaging device, operating at 8 MHz, that was capable of detecting bubbles greater than 10 μm in diameter. The results showed that bubbles were formed for I_{SATA} intensities of 80 mW/cm^2 and their number increased with intensity. Subsequent theoretical studies suggest these bubbles were formed by rectified diffusion (*110*).

The formation of bubbles during decompression sickness also suggests the existence of *in vivo* cavitation nuclei. Factors that influence bubble formation in decompression studies include the following: Bubbles may sometimes form in supersaturated solutions by friction, a process called tribonucleation (*111*). This explains why limb movement has been shown in numerous studies to effect bubble formation. Bubbles may also form from pre-existing gaseous nuclei, particularly in adipose tissue. This factor has been used to explain why obesity can be correlated to the incidence and severity of decompression sickness, and why extravascular bubbles have been observed in adipose tissue during decompression sickness. Reynolds cavitation induced by turbulent flow and nuclear fission, due to cosmic radiation, have also been postulated as sources of bubbles *in vivo*.

Other evidence suggests that certain biological materials are resistant to bubble formation. Harvey et al., were unable to induce bubbles in the blood of cats, rabbits and dogs by rapid decompression, suggesting that at least for blood, few inhomogeneities exist to serve as cavitation nuclei (*112*).

The question of ultrasonically induced cavitation remains unresolved. A recent NIH consensus development conference on ultrasound imaging during pregnancy reaffirmed the use of ultrasound examinations when medically indicated (*113*). Clinical experience suggests any adverse effects have a low frequency of occurrence, a long latency period, or both. The chemical similarities between ionizing radiation and ultrasonic exposure are interesting and perhaps should raise our level of concern. Decompression studies suggest that if ultrasonic cavitation does occur *in vivo*, it may be tissue-specific; (fat may be more susceptible than blood) and it may be influenced by motion and radiation. Even if cavitation occurs *in vivo*, its outcome is unknown. Per-

haps epidemiological studies will be needed to ultimately determine the risk associated with ultrasonic exposure.

Conclusion

Free radicals play a significant role in the sonochemistry of both aqueous and nonaqueous solutions. Their formation is a consequence of the dynamic forces of cavitation and results from thermal decomposition of molecules in the high temperature zones of collapsing bubbles as described by the modified Noltingk-Neppiras "hot spot" theory. Free-radical intermediates have been inferred from product studies, demonstrated by the use of chemical probes and identified by spin trapping and ESR techniques. Although certain differences exist between sonochemistry and ionizing radiation chemistry, the number of similarities is striking.

The experimental techniques used in ultrasonic research pose a number of challenges. The results obtained to date ensure that this field will continue to experience high interest and activity because of its significance to a wide assortment of disciplines encompassing large areas of physical science, medicine and engineering.

REFERENCES

1. Flynn, H. G. Physics of acoustic cavitation in liquids. In: Physical Acoustics, Vol. 1B (W. P. Mason, Ed.), Academic Press, New York, 1964, pp. 57–172.
2. Apfel, R. E. Acoustic cavitation. In: Ultrasonics (P. D. Edmonds, Ed.), Vol. 19 of series, Methods of Experimental Physics (C. Marton, Ed.), Academic Press, New York, 1981, pp. 355–411.
3. AIUM-NEMA (1981). AIUM-NEMA safety standard for diagnostic ultrasound equipment, AIUM-NEMA Publication UL 1-1981, Washington, D C; J. Ultrasound Med. (Suppl.) 2(2): April 1983.
4. Coakley, W. T., and Nyborg, W. L. Cavitation; dynamics of gas bubbles; applications. In: Ultrasound: Its Applications in Medicine and Biology (F. J. Fry, Ed.), Elsevier, New York, 1978, pp. 77–159.
5. Basedow, A. M., and Ebert, K. H. Ultrasonic degradation of polymers in solution. In: Advances in Polymer Science, Vol. 22 (H. J. Cantow et al., Eds.), Springer-Verlag, New York, 1977, pp. 83–148.
6. Neppiras, E. A. Acoustic cavitation series: part one. Acoustic cavitation: an introduction. Ultrasonics, 22: 25–28 (January 1984).
7. Apfel, R. E. The tensile strength of liquids. Sci. American 227(6): 58–71, 1972.
8. Greenspan, M., and Tschiegg, C. E. Radiation-induced acoustic cavitation; apparatus and some results. J. Res. Natl. Bur. Stand. 71C: 299–312 (1967).
9. Apfel, R. E. A novel technique for measuring the strength of liquids. J. Acoust. Soc. Am. 49: 145–155 (1971).
10. Crum, L. A. Nucleation and stabilization of microbubbles in liquids. Appl. Sci. Res. 38: 101–115 (1982).
11. Apfel, R. E. Acoustic cavitation series: part four. Acoustic cavitation inception. Ultrasonics 22: 164–173 (July 1984).
12. Apfel, R. E. The role of impurities in cavitation-threshold determination. J. Acoust. Soc. Am, 48: 1179–1186 (1970).
13. Crum, L. A. Acoustic cavitation thresholds in water. In: Cavitation Inhomogeneities in Underwater Acoustics, Springer-Verlag, New York, 1980, pp. 84–89.
14. Strasberg, M. Onset of ultrasonic cavitation in tap water. J. Acoust. Soc. Am. 31: 163–176 (1959).
15. Fox, F. E., and Herzfeld, K. F. Gas bubbles with organic skin as cavitation nuclei. J. Acoust. Soc. Am. 26: 985–989 (1954).
16. Sirotyuk, M. G. Stabilization of gas bubbles in water. Sov. Phys. Acoustics 16: 237–240 (1970).
17. Sirotyuk, M. G. Elasticity and strength of stable gas bubbles in water. Sov. Phys. Acoustics 16: 482–484 (1971).
18. Yount, D. E. Skins of varying permeability: a stabilization mechanism for gas cavitation nuclei. J. Acoust. Soc. Am. 65: 1429–1439 (1979).
19. Seitz, F. On the theory of the bubble chamber. Phys. Fluids 1: 2-13 (1958).
20. Lauterborn, W. Zu einer Theorie der Kavitationsschwellen. Acustica 22: 48–54 (1969/1970).
21. Noltingk, B. E., and Neppiras, E. A. Cavitation produced by ultrasonics. Proc. Phys. Soc. (London), B63: 674–685, 1950.
22. Miller, D. L. The design, construction and testing of an in vivo cavitation detector. Proposal for USFDA Contract 223-79-6015, DHHS, Rockville, MD, 1979, p. 17.
23. Crum, L. A. Measurements of the growth of air bubbles by rectified diffusion. J. Acoust. Soc. Am. 68: 203–211 (1980).
24. Flynn, H. G. Generation of transient cavities in liquids by microsecond pulses of ultrasound. J. Acoust. Soc. Am. 72: 1926–1932 (1982).
25. Frenkel, Ya. I. On the electrical effects connected with cavitation caused by ultrasonic oscillations in a liquid. J. Phys. Chem. (USSR), 14: 305–308 (1940).
26. Griffing, V. The chemical effects of ultrasonics. J. Chem. Phys. 20: 939–942 (1952).
27. Saksena, T. K., and Nyborg, W. L. Sonoluminescence from stable cavitation. J. Chem. Phys. 53: 1722–1734 (1970).
28. Young, F. R. Sonoluminescence from water containing dissolved gases. J. Acoust. Soc. Am. 60: 100–104 (1976).
29. Sehgal, C., Sutherland, R. G., and Verrall, R. E. Optical spectra of sonoluminescence from transient and stable cavitation in water saturated with various gases, J. Phys. Chem. 84: 388–395 (1980).
30. Sehgal, C., Steer, R. P., Sutherland, R. G., and Verrall, R. E. Sonoluminescence of argon saturated alkali metal salt solutions as a probe of acoustic cavitation. J. Chem. Phys. 70: 2242–2248 (1979).
31. Flynn, H. G., and Church, C. C. A mechanism for the generation of cavitation maxima by pulsed ultrasound. J. Acoust. Soc. Am. 76: 505–512 (1984).
32. O'Brien, W. O., Jr., Christman, C. L., and Yarrow, S. Ultrasonic biological effect exposure system, Ultrasonic Symp. Proc. IEEE, CHO 896-ISU, 57–64, 1974.
33. Henglein, A., and Schulz, R. Der Einfluss organischer Verbindungen auf einige chemische Wirkungen des Ultraschalls. Z. Naturforschung 8: 277–284 (1953).
34. Church, C. C., Flynn, H. G., Miller, M. W., and Sachs, P. G. The exposure vessel as a factor in ultrasonically-induced mammalian cell lysis. II. Ultrasound Med. Biol. 8: 299–309 (1982).
35. McKee, J. R., Christman, C. L., O'Brien, W. D., Jr. and Wang, S. Y. Effects of ultrasound on nucleic acid bases. Biochemistry 16: 4651–4654 (1977).
36. Armour, E. P., and Corry, P. M. Cytotoxic effects of ultrasound in vitro dependence on gas content, frequency, radical scavengers, and attachment. Radiat. Res. 89: 369–380 (1982).
37. Esche, R. Untersuchungen der Schwingungskavitation in Flüssigkeiten. Acustica 2: 208–218 (1952).
38. El'piner, I. E. Ultrasound: Physical, Chemical and Biological Effects. Consultants Bureau, New York, 1964.
39. Spinks, J. W. T., and Woods, R. J. An Introduction to Radiation Chemistry, 2nd Ed., John Wiley and Sons, New York, 1976.
40. Draganić, I. G., and Draganić, Z. D. The Radiation Chemistry of Water. Academic Press, New York, 1971.
41. Margulis, M. A. Cavitation-diffusion model of the spatial dis-

tribution of radicals in an ultrasonic field. Russ. J. Phys. Chem. 50: 534–537 (1976).
42. Miller, N. Chemical action of sound waves on aqueous solutions. Trans. Faraday Soc. 46: 546–549 (1950).
43. Henglein, A., and Schulz, R. Die Auslösung der Polymerisation des Acrylamids durch Ultraschall. Z. Naturforsch. 7: 484–485 (1952).
44. Henglein, A. Die Beschleunigung chemischer Reaktionen des Ultraschalls in Lösungen von Sauerstoff-Edelgas-Gemischen. Naturwiss. 43: 277 (1956).
45. Weissler, A. Formation of hydrogen peroxide by ultrasonic waves: free radicals. J. Am. Chem. Soc. 81: 1077–1081 (1958).
46. Anbar, M., and Pecht, I. On the sonochemical formation of hydrogen peroxide in water. J. Phys. Chem. 68: 352–355 (1964).
47. Anbar, M., and Pecht, I. The sonolytic decomposition of organic solutes in dilute aqueous solutions. I. Hydrogen abstraction from sodium formate. J. Phys. Chem. 68: 1460–1462 (1964).
48. Mead, E. L., Sutherland, R. G., and Verrall, R. E. The ultrasonic degradation of thymine. Can. J. Chem. 53: 2394–2399 (1975).
49. Sehgal, C. M., and Wang, S. Y. Threshold intensities and kinetics of sonoreaction of thymine in aqueous solutions at low ultrasonic intensities. J. Am. Chem. Soc. 103: 6606–6611 (1981).
50. Wang, S. Y., and Gupta, A. B. Effect of pulse ultrasound on nucleic acid components. 1977 Ultrasonics Symposium Proceedings, IEEE Cat. #77 CH1264-ISU.
51. Sehgal, C. M., and Wang, S. Y. Chemical dosimetry for the measurement of transient cavitation activity. IEEE Transactions on Sonics and Ultrasonics SU-30: 374–379 (1983).
52. Weissler, A. Some sonochemical reaction yields. J. Acoust. Soc. Am. 32: 283–284 (1960).
53. Makino, K., Mossoba, M. M., and Riesz, P. Chemical effects of ultrasound on aqueous solutions. Evidence for ·OH and ·H by spin trapping. J. Am. Chem. Soc. 104: 3537–3539 (1982).
54. Makino, K., Mossoba, M. M., and Riesz, P. Chemical effects of ultrasound on aqueous solutions. Formation of hydroxyl radicals and hydrogen atoms. J. Phys. Chem. 87: 1369–1377 (1983).
55. Janzen, E. G. A critical review of spin trapping in biological systems. In: Free Radicals in Biology, Vol. IV (W. A. Pryor, Ed.), Academic Press, New York, 1980, pp. 116–154.
56. Aurich, H. G. Nitroxides. In: Supplement F, The Chemistry of Amino, Nitroso, and Nitrocompounds and Their Derivatives, Part I (S. Patai, Ed.), John Wiley and Sons, New York, 1982.
57. Kalyanaraman, B. Detection of toxic free radicals in biology and medicine. In: Reviews of Biochemical Toxicology, Vol. IV (E. Hodgson, J. R. Bend, and R. M. Philpot, Eds.), Elsevier, New York, 1982.
58. Riesz, P., and Rustgi, S. Aqueous radiation chemistry of protein and nucleic constituents: ESR and spin-trapping studies. Radiat. Phys. Chem. 13: 21–40 (1979).
59. Riesz, P., and Rosenthal, I. Photochemistry of protein and nucleic acid constituents: electron spin resonance and spin trapping with 2-methyl-2-nitrosopropane. Can. J. Chem. 60: 1474–1479 (1982).
60. Rosenthal, I., Mossoba, M. M., and Riesz, P. Sonolysis of perhalomethane as studied by EPR and spin trapping. J. Mag. Reson. 45: 359–361 (1981)
61. Carmichael, A. J., Makino, M. M., and Riesz, P. Quantitative aspects of ESR and spin trapping of hydroxyl radicals and hydrogen atoms in gamma-irradiated aqueous solutions. Radiat. Res. 100: 222–234 (1984).
62. Neta, P., Steenken, S., Janzen, E. G., and Shetty, R. V. Pattern of addition of hydroxyl radicals to the spin traps of α-pyridyl-1-oxide N-tert butyl nitrone. J. Phys. Chem. 84: 532–534 (1980).
63. Finkelstein, E., Rosen, G. M., and Rauckman, E. J. Spin trapping of superoxide and hydroxyl radical: practical aspects. Arch. Biochem. Biophys. 200: 1–16 (1980).
64. Janzen, E. G., Wang, Y. Y., and Shetty, R. V. Spin trapping with α-pyridyl-1-oxide N-tert-butyl nitrones in aqueous solutions. A unique electron spin resonance spectrum for the hydroxyl radical adduct. J. Am. Chem. Soc. 100: 2923–2925 (1978).
65. Kalyanaraman, B., Felix, C. C., and Sealy, R. C. Photoionization of melanin precursors. An electron spin resonance investigation using the spin trap 5,5 dimethyl-l-pyrroline-1-oxide (DMPO). Photochem. Photobiol. 36: 5–12 (1982).,
66. Makino, K., Mossoba, M. M., and Riesz, P. Formation of •OH and •H in aqueous solutions by ultrasound using clinical equipment. Radiat. Res. 96: 416–421 (1983).
67. Christman, C. L., Carmichael, A. J., Mossoba, M. M., and Riesz, P. Detection of transient cavitation in aqueous solutions exposed to microsecond pulses of ultrasound. 32nd Annual Meeting of the Radiation Research Society, Orlando, Florida, March, 1984.
68. Edmonds, P. D., and Sancier, K. M. Evidence for free radical production by ultrasonic cavitation in biological media. Ultrasound Med. Biol. 9: 635–639 (1983).
69. Rehorek, D., and Janzen, E. G. Ueber den Nachweis von Radikalen bei der Sonolyse von $[Co(NH_3)_5N_3]Cl_2$. Z. Chem. 24: 228–229 (1984).
70. Fitzgerald, M. E., Griffing, V., and Sullivan, J. Chemical effects of ultrasonics—"hot spot" chemistry. J. Chem. Phys. 25: 926–933 (1956).
71. Niemczewski, B. A. comparison of ultrasonic cavitation intensity in liquids. Ultrasonics 18: 107–110 (1980).
72. Luche, J. L., and Damiano, J. C. Ultrasound in organic synthesis. I. Effect on the formation of lithium organometalic reagents. J. Am. Chem. Soc. 102: 7926–7927 (1980).
73. Han, B. H., and Boudjouk, P. Organic sonochemistry. Ultrasound-promoted coupling of organic halides in the presence of lithium wire. Tetrahedron Letters 22: 2757–2758 (1981).
74. Boudjouk, P., and Han, B. H. Organic sonochemistry. Ultrasound-promoted coupling of chlorosilanes in the presence of lithium wire. Tetrahedron Letters 22: 3813–3814 (1981).
75. Schultz, R., and Henglein, A. Ueber den Nachweiss von freien Radikalen, die unter dem Einfluss von Ultraschallwellen gebildet werden, mit Hilfe von Radical-Kettenpolymerisation und Diphenyl-pikryl-hydrazyl. Z. Naturforsch. 8b: 160–161 (1953).
76. Weissler, A., Pecht, I., and Anbar, M. Ultrasound chemical effects on pure organic liquids. Science 150: 1288–1289 (1965).
77. Suslick, K. S., and Schubert, P. F. Sonochemistry of $Mn_2(CO)_{10}$ and $Re_2(CO)_{10}$. J. Am Chem. Soc. 105: 6042–6044 (1983).
78. Suslick, K. S., Gawienowski, J. J., Schubert, P. F., and Wang, H. H. Alkane sonochemistry. J. Phys. Chem. 87: 2299–2301 (1983).
79. Suslick, K. S., Schubert, P. F., and Goodale, J. W. Sonochemistry and sonocatalysis of iron carbonyls. J. Am. Chem. Soc. 103: 7342–7344 (1981).
80. Suslick, K. S., Goodale, J. W., Schubert, P. F., and Wang, H. H. Sonochemistry and sonocatalysis of metal carbonyls. J. Am. Chem. Soc. 105: 5781–5785 (1983).
81. Suslick, K. S., Schubert, P. F., and Goodale, J. W. Chemical dosimetry of ultrasound cavitation. IEEE Ultrasound Symp. 612–616 (1981).
82. Suslick, K. S., Gawienowski, J. J.., Schubert, P. F., and Wang, H. H. Sonochemistry in non-aqueous liquids. Ultrasonics 22: 33–36 (1984).
83. Rehorek, D., and Janzen, E. G. Spin trapping of radicals generated by ultrasonic decomposition of organotin compounds. J. Organomet. Chem. 268: 135–139 (1984).
84. Toy, M. S., and Stringham, R. S. Ultrasonic photolysis of methyl disulfide and hexafluorobutadiene. J. Fluor. Chem. 25: 213–218 (1984).
85. Diedrich, G. K., Kruus, P., and Rachlis, L. M. Cavitation-induced reactions in pure substituted benzenes. Can. J. Chem. 50: 1743–1750 (1972).
86. Donaldson, D. J., Farrington, M. D., and Kruus, P. Cavitation-induced polymerization of nitrobenzene. J. Phys. Chem. 83: 3130–3135 (1979).
87. Kruus, P. Polymerization resulting from cavitation. Ultrasonics 21: 201–204 (1983).
88. Kopina, I. V., Korneeva, O. G., Konoenko, G. G., and Malkes, L. Y. Comparative characteristics of polystyrene prepared by ultrahigh-frequency and thermal initiation. Deposited Doc. SPSTL 362khp-D81 (1981); Chem. Abstr. 97: 145370b (1982).
89. Fujiwara, H., and Kunio, G. Copolymerization in mixtures of aluminum acetyl-acetonate, styrene and methyl methacrylate by ultrasonic irradiation. Kobunshi Ronbunshu 39: 481–485 (1982).

90. Henglein, A. Die Reaktion des α, α '-Diphenyl-β-pikryl-hydrazyls mit langkettigen freien Radikalen, die beim Ultraschallabbau von Polymethacrylsäuremethylester gebildet werden. Makromol. Chem. 15: 188–210 (1955).
91. Henglein, A. Die Kombination von freien makromolekularen Radikalen, die durch Ultraschallabbau von Polymethacrylsäuremethylester und von Polystyrol gebildet werden. Makromol. Chem. 18: 37–47 (1956).
92. Henglein, A. Die Reaktion von Jod mit langkettigen freien Radikalen, die durch Ultraschall-Abbau des Polymethacrylsäuremethylesters entstehen. Z. Naturforsch. 10b: 953–960 (1955).
93. Fujiwara, H., Okazaki, K., and Goto, K. Mechanochemical reaction of polymers by ultrasonic irradiation. 1. Mechanochemical reaction in mixtures of poly-styrene, styrene, and solvents. J. Polym. Sci. Polym., Phys. Ed. 13: 953–960 (1975).
94. Fujiwara, H., Kimura, K., Mori, H., and Goto, K. Mechanochemical reaction of polymers by ultrasonic irradiation. 5. Mechanochemical copolymerization in mixtures of poly (vinyl chloride), styrene and solvents. Polym. J. 13: 927–933 (1981).
95. O'Driscoll, K. F., and Sridharah, A. U. Effect of ultrasound on free-radical polymerization in a continuous stirred tank reactor. J. Polym. Sci. Polym. Chem. Ed. 11: 1111–1117 (1984).
96. Malhotra, S. L., and Gauthier, J. M. Ultrasonic modification of polymers. I. Degradations of polystyrene in the presence of various poly (alkyl methylates). J. Macromol. Sci.–Chem. A18: 783–816 (1982).
97. Allen, P. E. M., Downer, J. M., Hastings, G. W., Melville H. W., Molyneux, P., and Urwin, J. R. New methods of preparing block copolymers. Nature 177: 910–912 (1956).
98. Tabata, M., Miyazawa, T., Kobayashi, O., and Sohma, J. Direct evidence of main-chain scissions induced by ultrasonic irradiation of benzene solutions of polymers. Chem. Phys. Letters 73: 178–180 (1980).
99. Tabata, M., and Sohma, J., Spin trapping studies of poly (methyl methacrylate) degradation in solution. Eur. Polym. J. 16: 589–595 (1980).
100. Hall, E. J. Radiobiology for the Radiologist. Harper and Row, Philadelphia, 1978.
101. Roots, R, and Okada, S. Protection of DNA molecules in cultured mammalian cells from radiation-induced single-strand scissions by various alcohols and SH compounds. Int. J. Rad. Biol. 21: 329–342 (1972).
102. Roots, R., and Okada, S. Estimation of life times and diffusion distances of radicals involved in x-ray induced DNA strand breaks or killing of mammalian cells. Radiat. Res. 64: 306–320 (1975).
103. Chapman, J. D., Reuvers, A. P., Borsa, J. and Greenstock, C. L. Chemical protection and radiosensitization of mammalian cells growing *in vitro*. Radiat. Res. 56: 291–306 (1973).
104. Samuni, A. Chevion, M., and Czapski, G. Roles of copper and O_2 in the radiation-induced inactivation of T7 bacteriophage. Radiat. Res. 99: 562–572 (1984).
105. Johnson, J., and Abernathy, D. L. Diagnostic imaging procedure volume in the United States. Radiology 146: 851–853 (1983).
106. Carson, P. L., Fischella, P. R., and Oughton, T. V. Ultrasonic power and intensities produced by diagnostic ultrasound equipment. Ultrasound Med. Biol. 3: 341–350 (1978).
107. Apfel, R. E. Acoustic cavitation: a possible consequence of biomedical uses of ultrasound. Brit. J. Cancer 45 (Suppl V): 140–146 (1982).
108. Wells, P. N. T. Biomedical Ultrasonics. Academic Press, New York, 1977, p. 432.
109. ter Haar, G., and Daniels, S. Evidence for ultrasonically induced cavitation in vivo. Phys. Med. Biol. 26: 1145–1149 (1981).
110. Crum, I. A., and Hansen, G. M. Growth of air bubbles in tissue by rectified diffusion. Phys. Med. Biol. 27: 413–417 (1982).
111. McDonough, P. M., and Hemmingsen, E. A. Bubble formation in crabs induced by limb motions after decompression. J. Appl. Physiol. Respirat. Environ. Exercise Physiol. 57: 117–122 (1984).
112. Harvey, E. N., Whiteley, A. H., McElroy, W. D., Pease, D. C., and Barnes, D. K. Bubble formation in animals. II Gas nuclei and their distribution in blood and tissues. J. Cell. Comp. Physiol, 24: 24–34 (1944).
113. Gold, R. B. Ultrasound imaging during pregnancy. Fam. Plan. Perspect. 16: 240–243 (1984).